Cairo University

Faculty of Computers and Artificial intelligence

Information Technology Department

Brain Tumor Detection

By:

Mohamed Alaa Eldin Elkilany	20170245
Mohamed Hamdy Mohamed	20170227
Ahmad Gomma Farouk	20170014
Mohamed Ali Farouk	20170249

Supervised by: DR Mona Soliman

TA: Salah Mostafa Salah El Abyad

July 2021

Abstract:

Brain tumor is one of the most dangerous types of cancer caused by the 5-year survival rate is only about 36%. Accurate diagnosis of the brain the tumor is critical to treatment planning. A major challenge in brain tumor treatment planning and quantitative evaluation is determination of the tumor extent. The noninvasive magnetic resonance imaging (MRI) technique has emerged as a front-line diagnostic tool for brain tumors without dionizing radiation. Manual segmentation of brain tumor extent from 3D MRI volumes is a very time-consuming task and the performance is highly relied on operator's experience. In this context, a reliable fully automatic segmentation method for the brain tumor segmentation is necessary for an efficient measurement of the tumor extent. In this study, we propose two a fully automatic method for brain tumor segmentation, which is developed using U-Net based model and convent based model deep convolutional networks. Automatic segmentation of brain tumors from medical images is important for clinical assessment and treatment planning of brain tumors. Recent years have seen an increasing use of convolutional neural networks (CNNs) for this task, but most of them use either 2D networks with relatively low memory requirement while ignoring 3D context, or 3D networks exploiting 3D features while with large memory consumption. In addition, existing methods rarely provide uncertainty information associated with the segmentation result. We propose a cascade of CNNs to segment brain tumors with hierarchical sub-regions from multi-modal Magnetic Resonance images (MRI), and introduce a 2.5D network that is a trade-off between memory consumption, model complexity and receptive field. In addition, we employ test-time augmentation to achieve improved segmentation accuracy, which also provides voxel-wise and structure-wise uncertainty information of the segmentation result. Experiments with BraTS'2017 dataset showed that our cascaded framework with 2.5D CNNs was one of the top performing methods (second-rank) for the BraTS challenge. We also validated our method with BraTS'2018 dataset and found that test-time augmentation improves brain tumor segmentation accuracy and that the resulting uncertainty information can indicate potential mis-segmentations and help to improve segmentation accuracy.

Table of Contents

1. Introduction	**9**
1.1 Overview	**9**
1.2 Problem Definition	**10**
1.3 Motivation and Objective	**12**
1.4 methodology of the project	**13**
2. Related Work	**14**
2.1 A Survey on Brain Tumor Detection Based on Structural MRI Using Machine Learning and Deep Learning Techniques.	**14**
2.2 Automatic Brain Tumor Segmentation	**15**
2.3 Deep Convolutional Neural Networks Using U-Net for Automatic Brain Tumor Segmentation in Multimodal MRI Volumes	**15**
2.4 Multimodal Brain Tumor Segmentation Using Cascaded V-Nets	**16**
2.5 Tumor Segmentation and Survival Prediction in Glioma with Deep Learning	**18**
3. Basic knowledge	**22**
3.1- deep learning	**22**
3.1.1-CNN	**22**
3.2- medical knowledge of BTD	**24**
4. The Proposed models for brain tumor segmentation	**25**
4.1-introduction	**25**

4.2- Data Collection phase	26
4.3-preprocessing phase	26
4.4-training phase	28
4.4.1- U-net brain segmentation based model	28
4.4.2- convent brain segmentation based model	31
4.5- Prediction phase	32
5. Result Analysis	34
5.1- segmentation result	34
5.1.1- U-net brain segmentation based model	34
5.1.2- convent brain segmentation based model	49
5.2- classification result	55
5.3- implementation analysis	57
5.4- comparative analysis	59
6. Conclusion	60
7. Future work	61
8. References	62

List of figures

fig .1: shows the comparison of deferent algorithms and the accuracy of each one 12	14
fig.2 shows the training architecture for the V-net model	16
fig.3 shows the testing architecture for the V-net model	18
fig.4 shows the over view of the model	18
fig.5 show the Cascaded framework and architecture of CA-CNN	19
fig.6 shows the Architecture of DFKZ Net.	20
fig.7 shows the feature extraction phase.	21
fig.8 show the flow of the model.	25
fig.9 show the preprocessing flowchart	27
fig. 10. Architecture of the proposed Deep Convolutional Neural Network.	29
fig.11 Show the training flowchart	30
fig.12 Multi-planar ConvNet architecture for segmentation.	31
fig. 13. Show the Model 2 flowchart.	32
fig. 14. Show the prediction flowchart	33
fig.15 shows the t1 coronal view	34
fig.16 shows the t1c coronal view	34
fig.17 shows the t2 coronal view	34
fig.18 shows the flair coronal view	34
fig.19 shows the ground truth coronal view	35
fig.20 shows the prediction coronal view	35
fig.21 shows the final GUI prediction coronal view	35
fig22. shows the t1 sagittal view	36
fig.23 shows the t1c sagittal view	36
fig.24 shows the t2 sagittal view	36
fig.25 shows the flair sagittal view	36
fig.26 shows the ground truth sagittal view	37

fig.27 shows the prediction sagittal view	37
fig.28 shows the final GUI prediction sagittal view	37
fig.29 shows the t1 axial view	38
fig.30 shows the t2 axial view	38
fig.31 shows the t1c axial view	38
fig.32 shows the flair axial view	38
fig.33 shows the ground truth axial view	39
fig.34 shows the prediction axial view	39
fig.35 shows the final GUI prediction axial view	39
fig.36 shows the t1 coronal view	40
fig.37 shows the t1c coronal view	40
fig.38 shows the t2 coronal view	40
fig.39 shows the flair coronal view	40
fig.40 shows the ground truth coronal view	41
fig.41 shows the prediction coronal view	41
fig.42 show the final GUI prediction Coronal view	41
fig.43 shows the t1 sagittal view	42
fig.44 shows the t1c sagittal view	42
fig.45 shows the t2 sagittal view	42
fig.46 shows the flair sagittal view	42
fig.47 shows the ground truth sagittal view	43
fig.48 shows the prediction sagittal view	43
fig.49 shows the final GUI prediction sagittal view	43
fig.50 shows the t1 sagittal view	44
fig.51 shows the t1c sagittal view	44
fig.52 shows the t2 sagittal view	44
fig.53 shows the flair sagittal view	44

fig.54 shows the ground truth sagittal view	45
fig.55 shows the prediction sagittal view	45
fig.56 shows the final GUI prediction sagittal view	45
fig.57 shows the accuracy of the first model.	46
fig.58 shows the loss of the first model.	46
fig.59 shows the precision of the first model.	47
fig.60 show the recall of the first model	47
fig.61 shows the f_score of the first model.	48
fig.62 shows the flair coronal view	49
fig.63 shows the prediction coronal view	49
fig.64 shows the flair sagittal view	49
fig.65 shows the prediction sagittal view	49
fig.66 shows the flair axial view	50
fig.67 shows the prediction axial view	50
fig.68 shows the flair coronal view	50
fig.69 shows the prediction coronal view	50
fig.70 shows the flair sagittal view.	51
fig.71 shows the prediction sagittal view.	51
fig.72 shows the flair axial view.	51
fig.73 shows the prediction axial view.	51
fig.74 shows the accuracy of the second model.	52
fig.75 shows the loss function of the second model.	52
fig.76 shows the precision of the second model.	53
fig.77 shows the recall of the second model.	53
fig.78 shows the f_score of the second model.	54
fig.79 shows this patent doesn't have tumor.	55
fig.80 shows patient has a tumor and this is its parts.	55

fig.81 shows the Confusion matrix of the first model	56
fig.82 shows the confusion matrix of the second model	56
fig.83 shows the main screen from the project GUI.	58

List of tables

Table. 1 shows the comparison between the different models.	60

1.Introduction

1.1 Overview

Brain tumor is considered one of the most severe diseases in medical science. Effective and efficient analysis is always a major concern of the radiologist in the early stage of tumor growth. Histological grading, based on stereotaxic biopsy testing, is the gold standard and convention for detecting the grade of a brain tumor. There are many risk factors involved in a biopsy test, including bleeding from the tumor and brain causing infection, seizures, severe migraines, stroke, coma and even death. But the main concern of stereotaxic biopsy is that it is not 100% accurate which can lead to serious diagnostic error followed by wrong clinical management of the disease.

Tumor biopsy being challenging for brain tumor patients, non-invasive imaging techniques like Magnetic Resonance Imaging (MRI) have been extensively employed in diagnosing brain tumors. Therefore, development of systems for the detection and prediction of the grade of tumors based on MRI data has become necessary. But at first sight of the imaging modality like in Magnetic Resonance Imaging (MRI), the proper visualization of the tumor cells and its differentiation with its nearby soft tissues is somewhat difficult task which may be due to the presence of low illumination in imaging modalities or its large presence of data or several complexity and variance of tumors-like unstructured shape, viable size and unpredictable locations of the tumor.

Automated defect detection in medical imaging using machine learning has become the emergent field in several medical diagnostic applications. Its application in the detection of brain tumor in MRI is very crucial as it provides information about abnormal tissues which is necessary for planning treatment. Studies in the recent literature have also reported that automatic computerized detection and diagnosis of the disease, based on medical image analysis, could be a good alternative as it would save radiologist time and also obtain a tested accuracy. Furthermore, if computer algorithms can provide robust and quantitative measurements of tumor depiction, these automated measurements will greatly aid in the clinical management of brain tumors by freeing physicians from the burden of the manual depiction of tumors

The machine learning based approaches like Deep ConvNets in radiology and other medical science fields plays an important role to diagnose the disease in much simpler way as never done before and hence providing a feasible alternative to surgical biopsy for brain tumors . In this project, we attempted at detecting and classifying the brain tumor and comparing the results of binary and multi class classification of brain tumor with and without Transfer Learning (use of pre-trained Keras models) using Convolutional Neural Network (CNN) architecture.

1.2 Problem definition

One of the reasons for the rise in death rates in today's society is the development of brain tumors. Any mass caused by aberrant or uncontrolled cell development is referred to as a tumor. A benign or malignant brain tumor can exist. The structure of a benign brain tumor is uniform, and it does not contain active (cancer) cells, whereas the structure of a malignant brain tumor is non-uniform (heterogeneous), and it contains active cells. We must first read an MRI image of the brain before applying image segmentation to detect a brain tumor. We demonstrate an effective strategy for removing noise from MRI images and detecting brain malignancies

In general, the body consists of many types of cells, and each type has its own functions. The most cells in the body grow and divide in a regular manner to produce more cells. When the body needs it to maintain its health and safety of work. And when you lose your cells, its ability to control and discipline the process of its growth, and the rate of its division increases without any irregularity leading to the formation of extra cells of tissue called a tumor that can be benign or malicious

Possible causes of brain cancer:

Doctors have not yet come to know the causes that lead to tumors. The brain, and researchers are trying to discover it as this will improve the possibilities of discovery Means of prevention. Although doctors do not know an explanation for the injury of one person and not another with this kind of cancer, they know that these tumors do not spread from one person to another. Another because it is not contagious.

Brain tumors can affect people of all ages, but studies indicate that It is more common in two age groups, namely, children between the ages of 3 12 years and adults between 40 and 70 years old.

The researchers found, after studying the cases of large numbers of patients, that there are certain factors It increases the risk of a person developing a brain tumor at a higher rate than the average. For the sake of for example, some studies indicate that some types of brain tumors are more common. Workers in certain industries such as oil refining and the rubber and drug industries. In other studies indicated a higher rate of infection among pharmacists and embalmed with brain tumors. Researchers are also investigating exposure to viruses as one possible cause. The Brain tumors sometimes affect several members of the same family. The researchers are studying and Families who have had a number of brain tumors to know if genetics is the cause. Nor Scientists currently believe that head injuries lead to brain tumors

Symptoms of brain tumors:

Symptoms of brain tumors depend primarily on its size and location in the brain. The causes of symptoms are damage to vital tissues and pressure on the brain when the tumor grows within the limited space of the skull. It can also cause bloating it is caused by the accumulation of fluid around the tumor, and this condition is known as edema. And you can come back Symptoms also include hydrocephalus, which occurs when the tumor blocks the flow of cerebrospinal fluid. The sciatica, which causes it to build up in the ventricles, and a brain tumor can grow very slowly, the most common symptoms of brain tumors appear, A headache that is usually severe in the morning and relieves during the day.

• Epileptic seizures. • Nausea or vomiting.
• Weakness or numbness in the arms or legs.
• Stumbling or uncoordinated walking (a staggering gait).
• Abnormal movements of the eyes or changes in vision.
• Dizziness. • Changes in personality or memory.
• Changes in the way you speak**.**

Diagnosis

To find out the causes of the symptoms that appear on the patient, the doctor asks the doctor about his biography and ambassador He received his medical doctor, and he is undergoing a full medical examination. In addition to checking for health signs In general, the doctor will perform a neurological examination that includes tests for alertness and muscle strength. Coordination, reflexes and response to pain. The doctor also examines the patient's eyes to make sure the absence of swelling due to tumor pressure on the nerve that connects the eye to the brain.

Depending on the results of the medical and neurological examinations, the doctor may order one of the following examinations or both

1. Computer tomography (Scan CT): A series of detailed images of the brain. An electronic computer connected to an X-ray machine produces the images. In some cases, a special dye is injected into a vein before imaging, which helps show differences in brain tissue
2. Magnetic resonance imaging (MRI): is a method that gives images of the brain using a powerful magnet connected to an electronic computer. For this reason, it is particularly useful in diagnosing brain tumors because it can detect through the bones of the skull on the tissues beneath it. A special dye can be used to increase the likelihood of detecting a brain tumor

Processing methods

Brain tumors are treated with surgery, radiation and chemotherapy, and several can be used Methods according to the patient's needs, he may be referred to doctors who specialize in different types of treatment and working together as an African. This team often includes a neurosurgeon and a doctor. A cancer specialist, a nutritionist, and a social researcher. Can the patient also deals with physical therapy and occupational rehabilitation therapy?

Surgery: This is the standard treatment for most brain tumors. To remove a tumor from the brain, it is opened the neurosurgeon makes a hole in the skull and tries to remove the entire tumor without harming the vital brain tissue, the doctor removes all that can be removed from the tumor. And help Partial elimination relieves symptoms by reducing pressure on the brain and minimizing the size of the tumor that then needs to be treated with radiation or chemotherapy

There are some tumors that cannot be removed, so medical treatment is taken in cases like these. Biopsy only so that a small piece of the tumor is extracted for the purpose of identifying its type Cancerous tissue and determine how to treat it afterwards.

1.3Motivation and Objective

In medical imaging of a brain tumor, our major goal is to extract meaningful and trustworthy information from these images with the least amount of error feasible, and then to determine the tumor's area in the image. To assist medical personnel in determining the size and severity of the tumor in order to make the best treatment option. The goal of this research is to create an algorithm that uses convolutional neural networks and segmentation techniques to extract a tumor image from an MRI brain image.

1.4 methodology of the project

Mention each chapter specialized in explaining what is in the paper .In chapter 3, discusses the subject of Brain Tumor and the many methods for detecting and classifying them. In chapter 4, we review the method that we learned to do this project, medical knowledge of BTD and deep learning is a machine learning technique that teaches a computer to filter inputs (observations in the form of images, text, or sound) through layers in order to learn how to predict and classify information. Deep learning is inspired by the way that the human brain filters information, in chapter 5 discusses the stages of the proposed system are presented. The first stage is the dataset collection, the second stage is the preprocessing, the third stage is the train model, and the last stage is predict and test model. In chapter 6, discusses the results of our study like model accuracy loss recall precision and f-score for two models, both of which are different architectures for the CNN network used to identify brain Tumor. In chapter 7 shows a fully automated and accurate approach for segmenting entire brain tumors and intra-tumor regions using a 2D deep convolution neural network with two alternative topologies based on a well-known medical-image architecture. In both HGG and LGG,the CNN model was trained. In chapter 8 We'll make changes in the future to speed up the CNN learning phase, and we'll apply ensemble learning methodologies to improve segmentation performance. In chapter 9 The reference that we worked from in the project.

2. Related work

This paper [23] introduces the brain tumor problem and show the different ways to detection and classification of the tumor.

The detection approach has 4 phases

2.1.1 Preprocessing

2.1.2 Segmentation

2.1.3 Feature extraction

2.1.4 Classification

With deferent algorithms to each phase then the paper compares between the different algorithms in different datasets and show the accuracy of this algorithms.

Ref	Preprocessing, Segmentation	Features	Classification	Dataset	Accuracy
[1]	Image resizing and enhancement	GLCM,CNN	SVM	Local-Iraqi center of research.	99.30%
[3]	Morphological operation, pixel subtraction, Maximum entropy threshold segmentation	Morphological ,Intensity	Naive Bayes	REMBRANDT	94%
[4]	Single Image Super Resolution for image enhancement Segmentation-Maximum fuzzy entropy (MFE)	ResNet deep features	SVM	TCIA	95%
[7]	Min-max normalization, Resize 224*224	GoogleNet deep features	SVM,KNN	CE-MRI	SVM-97.8% KNN-98%
[14]	Median filter GA segmentation	GLCM	SVM	Harvard Medical Dataset	91.23%
[15]	OTSU Binarization K-means clustering	DWT	SVM	BRATS 2013,BRATS 2017,Midas	99%
[23]	Skull stripping-BSE Gaussian filtering, K-Means segmentation	GLCM, Intensity, shape	SVM	Local ,AANLIB and RIDER	98%
[25]	Image enhancement-DSR-AD ,OTSU segmentation	Tamura, LBP, GLCM, Gabor, Shape	SVM	Local	98%
[26]	Image enhancement-DSR-AD ,Global adaptive segmentation	RLCP	Naive Bayes	Local-JMCD,BRATS	96%
[29]	Median filter noise removal, Threshold based segmentation	GLCM	Adaboost	Public dataset	89.90%
[31]	Wiener filtering Histogram based segmentation	GLCM	G-K Fuzzy system	-	95%

fig .1: shows the comparison of deferent algorithms and the accuracy of each one

This paper [14] considers performing the segmentation slice by slice from the axial view. Thus, the model processes sequentially each 2D axial image (slice) where each pixel is associated with different image modalities namely; T1, T2, T1C and FLAIR. Like most CNN-based segmentation models [35, 13], the method predicts the class of a pixel by processing the M×M patch centered on that pixel. The input X of our CNN model is thus an M×M 2D patch with several modalities.

The main building block used to construct a CNN architecture is the convolutional layer. Several layers can be stacked on top of each other forming a hierarchy of features. Each layer can be understood as extracting features from its preceding layer into the hierarchy to which it is connected. A single convolutional layer takes as input a stack of input planes and produces as output some number of output planes or feature maps. Each feature map can be thought of as a topologically arranged map of responses of a particular spatially local nonlinear feature extractor (the parameters of which are learned), applied identically to each spatial neighborhood of the input planes in a sliding window fashion. In the case of a first convolutional layer, the individual input planes correspond to different MRI modalities (in typical computer vision applications, the individual input planes correspond to there, green and blue color channels). In subsequent layers, the input planes typically consist of the feature maps of the previous layer.

This paper [32] presents a fully automated and efficient brain tumor segmentation method based on 2D Deep Convolutional Neural Networks (DNNs) which automatically extracts the whole tumor and intra-tumor regions, including enhancing tumor, edema and necrosis, from pre-operative multimodal 3D-MRI.

Weighted Cross Entropy (WCE) and Generalized Dice Loss (GDL) were employed as a loss function, and the dataset was BraTS’2018 that contain 351 multimodal MRI volumes of different patients.

This paper [32] presents the V-net model for segment the brain tumors based on the BRTs 2018 dataset, V-Net was initially proposed to segment prostate by training an end-to-end CNN on MRI and with the following architecture

1- Preprocessing
2- Training
3- Testing and prediction

In the preprocessing phase first the image is normalized using histogram matching, second step is to apply bias field correction to the image, then apply affine alignment and keep doing all the 3 steps until all the dataset finish

The architecture of our V-Net is shown in the next Figure, the left side of V-Net reduces the size of the input by down-sampling, and the right side of V-Net recovers the semantic segmentation image that has the same size with input images by applying de-convolutions. By means of introducing residual function and skip connection, V-Net has better segmentation performance compared with classical CNN. By means of introducing the 3D kernel with a size of 1 * 1 * 1, the numbers of parameters in V-Net is decreased and the memory consumption is greatly reduced

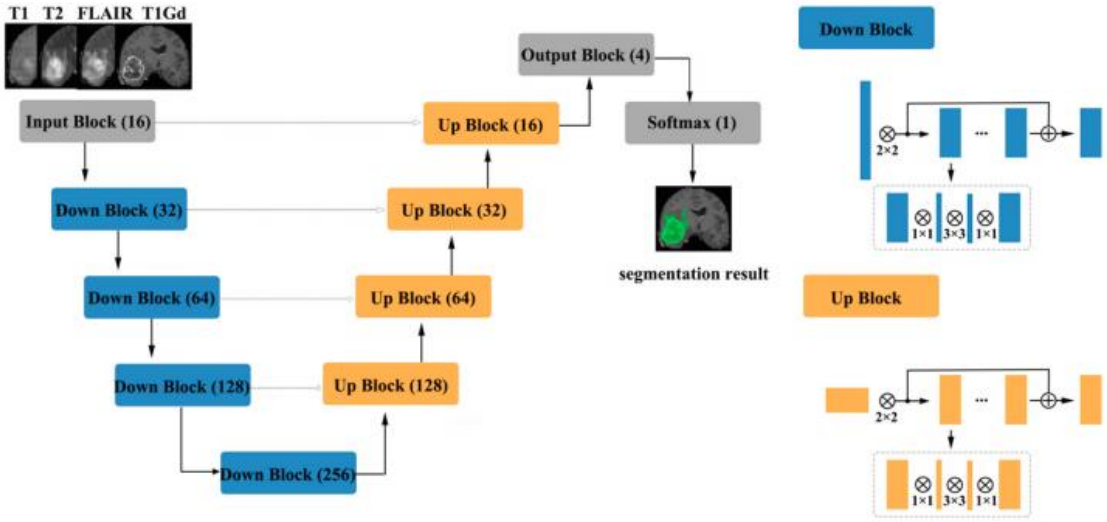

fig.2 shows the training architecture for the V-net model

Although V-Net has demonstrated promising performances in segmentation tasks, it could be further improved if incorporated with extra information, such as coarse localization. Therefore, the model proposes a cascaded V-Nets method for tumor segmentation. Briefly, first use one V-Net for the brain whole tumor segmentation, second use a second V-Net to further divide the tumor region into three substructures, e.g., tumor necrosis, edema, and enhancing tumor. Note that the coarse segmentation of whole tumor in the first V-Net is also used as receptive field to boost the performance. Detailed steps are as follows. The proposed framework is shown in the next Figure, there are two networks to segment substructures of brain tumors sequentially. The first network (V-Net 1) includes models 1–3, designed to segment the whole tumor. These models are trained by three kinds of preprocessed data mentioned in part of 2.1, respectively. V-Net 1 uses four modalities MR images as inputs, and outputs the mask of whole tumor (WT). The second network (V-Net 2) includes models 4-5, designed to segment the brain tumor into three substructures: tumor necrosis, edema, and enhancing tumor. These models are trained by the first two kinds of preprocessed data mentioned in part of 2.1, respectively. V-Net 2 also uses four modalities MR images as inputs, and outputs the segmented mask with three labels. Note that the inputs of V-Net 2 have been processed by using the mask of WT as region of interest (ROI). In other words, the areas out of the ROI are set as background. Finally, combine the segmentation results of whole tumor obtained by V-Net 1 and the segmentation results of tumor core (TC, includes tumor necrosis and enhancing tumor) obtained by V-Net 2 to achieve more accurate results about the three, The architecture of the used V-Net. 52 R. Hua et al.substructures of brain tumor. In short, the cascaded V-Nets take advantage of segmenting the brain tumor and three substructures sequentially, and ensemble of multiple models to boost the performance and achieve more accurate segmentation results

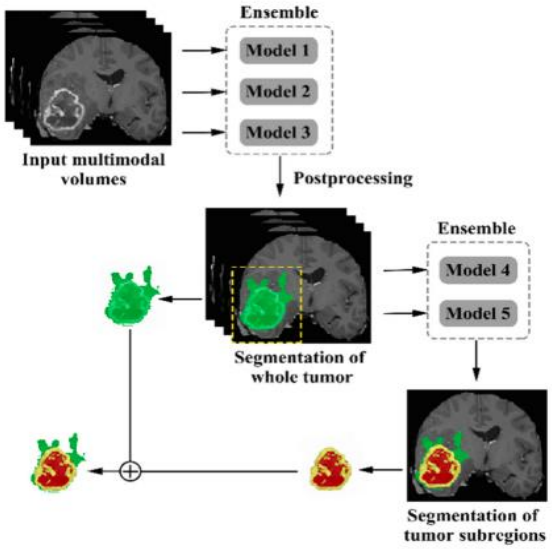

fig.3 shows the testing architecture for the V-net model

This paper [32] set the segmentation of the brain tumor according to the 3 phase's architecture

1- Preprocessing
2- Training
3- Testing

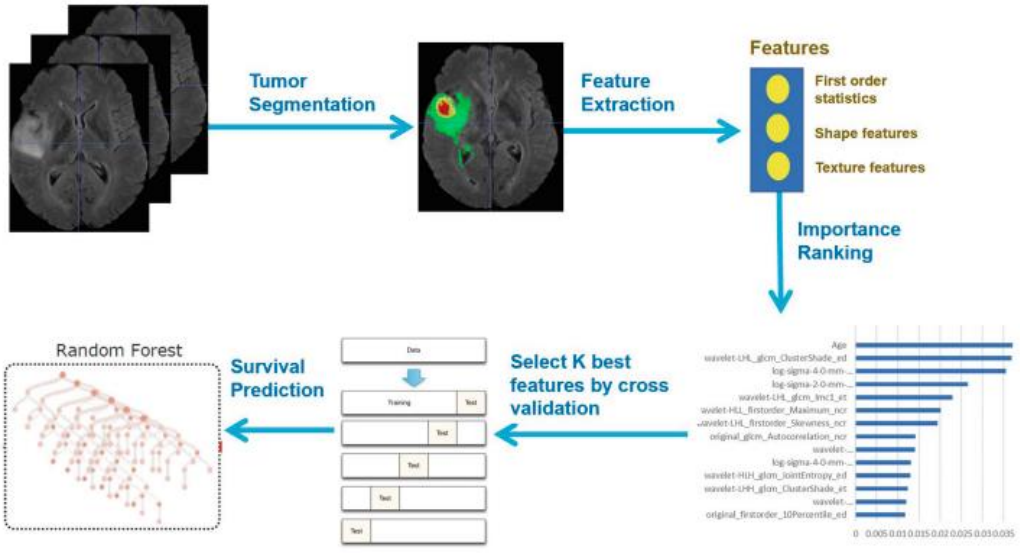

fig.4 shows the over view of the model

In the preprocessing phase apply the intensity normalization to reduce the bias in imaging. More specifically, the intensity value of each MRI is subtracted the mean and divided by the standard deviation of the brain region. In order to reduce over fitting, then applied random flipping and random Gaussian noise to augment the training set.

In order to perform accurate and robust brain tumor segmentation, we use an ensemble model comprising of three different convolutional neural network architectures. A variety of models have been proposed for tumor segmentation. Generally, they differ in model depth, filter number, connection way and others. Different model architectures can lead to different model performance and behavior. By training different kinds of model separately and merge the result, the model variance can be decreased and the overall performance can be improved. [11] We use three different CNN models and fuse the result by voting/majority rule. The detailed description of each model will be discussed as follows.86 L. Sun et al. CA-CNN. The first network we employ is Cascaded Anisotropic Convolutional Neural Network (CA-CNN) proposed by Wang et al. [17]. The cascade is used to convert multi-class segmentation problem into a sequence of three hierarchical binary segmentation problems. The network is illustrated as follows

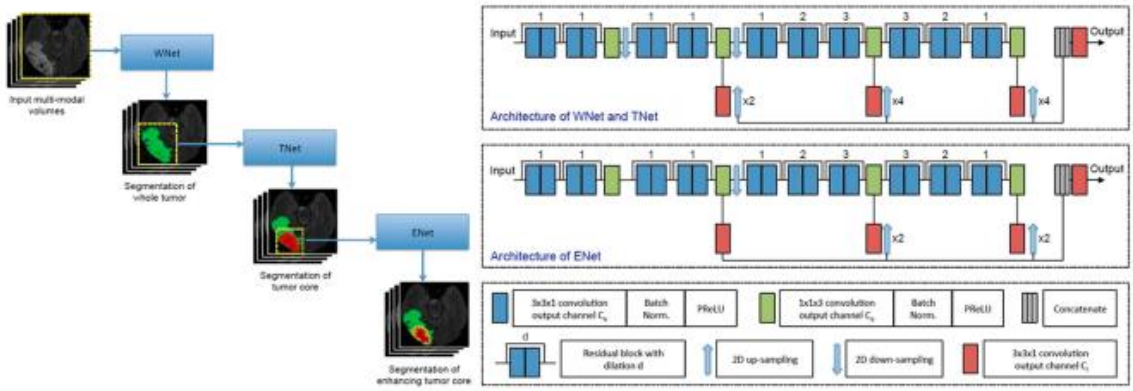

f*ig.5 show the Cascaded framework and architecture of CA-CNN*

The second network we employ is DFKZ Net, which was proposed by Isensee et al. [10] from German Cancer Research Center (DFKZ). This network is inspired by U-Net. It employs a context encoding pathway that extracts increasingly abstract representations of the input, and a decoding pathway used to recombine these representations with shallower features to precisely segment the structure of interest. The context encoding pathway consists of three content modules, each has two $3 \times 3 \times 3$ convolutional layers and a dropout layer with residual connection. The decoding pathway consists of three localization modules, each contains a $3 \times 3 \times 3$ convolutional layers followed by a $1 \times 1 \times 1$ convolutional layer. For the decoding pathway, the output of layers

of different depth is integrated by element wise summation, thus the supervision can be injected deep in the network

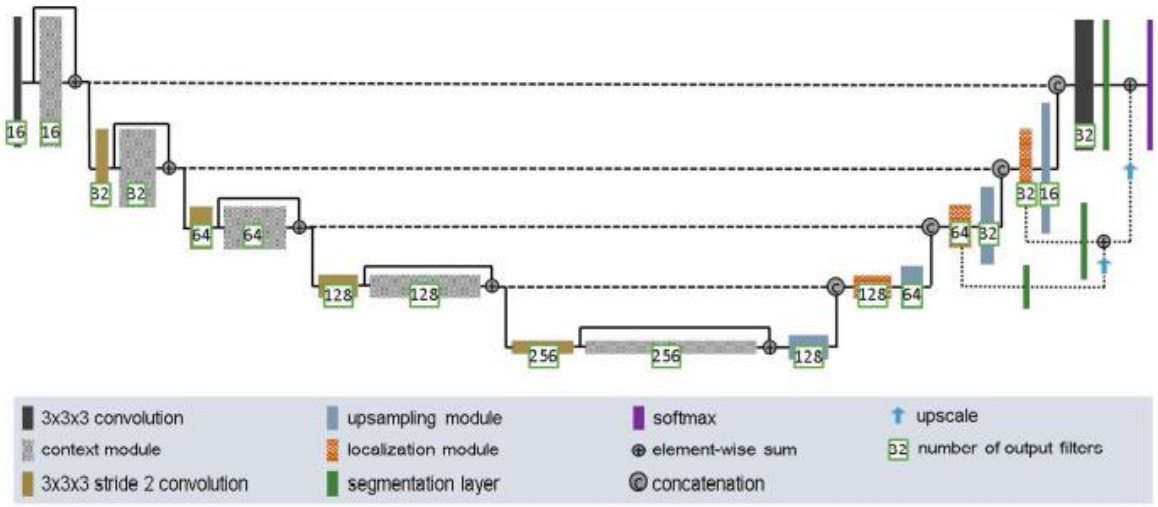

fig.6 shows the Architecture of DFKZ Net.

In feature extraction phase the Quantitative phenotypic features from MRI scans can reveal the characteristics of brain tumors. Based on the segmentation result, extract radiomics features from edema, non-enhancing solid core and necrotic/cystic core and the whole tumor region respectively using Pyradiomics toolbox, The modality used for feature extraction is depended on the intrinsic property of tumor sub region. For example, edema features are extracted from FLAIR modality, since it is typically depicted by hyper-intense signal in FLAIR. Non-enhancing solid core features are extracted from T1c modality, since the appearance of the necrotic (NCR) and the non-enhancing (NET) tumor core is typically hypo-intense in T1-Gd when compared to T1. Necrotic/cystic core tumor features are extracted from T1c modality, since it is described by areas that show hyper-intensity in T1Gd when compared to T1. The features we extracted can be grouped into three categories. The first category is first order statistics, which includes maximum intensity, minimum intensity, mean, median, 10th percentile, 90th percentile, standard deviation, variance of intensity value, energy, entropy and others. These features characterize the grey level intensity of tumor region. The second category is shape features, which include volume, surface area, surface area to volume ratio, maximum 3D diameter, maximum 2D diameter for axial, coronal and sagittal plane respectively, major axis length, minor axis length and least axis length, sphericity, elongation and other features. These features characterize the shape of tumor region. The third category is texture features, which include 22 grey level cooccurrence matrix (GLCM) features, 16 gray level run length matrix (GLRLM) features, 16 Grey level size zone matrix (GLSZM) features, five neighboring gray tone difference matrix (NGTDM) features and 14 gray level dependence matrix (GLDM) Features. These features characterize the texture of tumor region. Not only extract features from original images, but also extract features from Laplacian of Gaussian

(LoG) filtered images and images generated by wavelet decomposition. Because LoG filtering can enhance the edge of images, possibly enhance the boundary of tumor, and wavelet decomposition can separate images into multiple levels of detail components (finer or coarser). More specifically, from each region, 1131 features are extracted, including 99 features extracted from the original image, and 344 features extracted from Laplacian of Gaussian filtered images, since use 4 filters with sigma value 2.0, 3.0, 4.0, 5.0 respectively, and 688 features extracted from 8 wavelet decomposed images (all possible combinations of applying either a High or a Low pass filter in each of the three dimensions). In total, for each patient, we extract 1131 × 4 = 4524 radiomic features, these features are combined with clinical data (age and resection state) for survival prediction. The values of these features are normalized by subtracting the mean and scaling to unit variance.

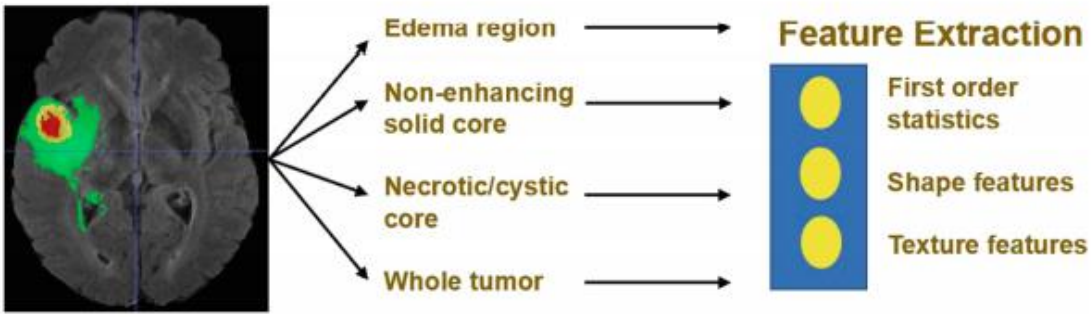

fig.7 shows the feature extraction phase.

3. Basic knowledge

3.1 Deep learning

Deep learning is a subset of machine learning, essentially a three or more-layered neural network. These neural networks try to imitate the human brain's behaviors, albeit not in line with its capacity, so it can "learn" from enormous quantities of data. While a single-layer neural network can predict approximately, further hidden layers can assist optimize and refine the accuracy.

The type of data with which it operates and the methods it learns differs from the standard machine learning.

Machine learning and profound learning models can also include several types of learning, which typically include supervised education, unattended learning and enhanced learning. Supervised learning uses tagged data sets to classify or predict, which means some form of intervention by human beings to appropriately label input data. Unattended learning, however, does not require labelled data sets and instead discovers patterns in the data, which are grouped together by any attributes. Reinforcement learning is a way to make a model more precise in an environment based on input, so that reward is maximized.

Deep neural networks consist of several layers of interconnected nodes, each built on the previous layers, for prediction or categorization to be improved and optimized. This development is known as propagation of calculations via the network. Visible layers are dubbed the input and output layers of a deep neural network. The entry layer is used to input the profound learning model for processing data and the end prevention or classification is performed in the output layer.

3.1.1 CNN

Classification and computer vision problems are more typically used by convolution neural networks (CNNs). In order to detect items on the images, manual and time-consuming approaches were utilised before CNNs. However, cool neural networks now give a scalable solution for the classification of the image and the recognition of objects, using linear algebra concepts, especially matrix multiplication, to find patterns inside an image. In this respect, they can be computer-intensive, requiring GPUs to train models.

The higher performance with picture, speech or audio signal inputs distinguishes convolution neural networks from other neural networks. It has three primary layer kinds, which are:

- Convolutional layer
- Pooling layer
- Fully-connected (FC) layer

The convolutional layer is the first layer of a convolutional network. While convolutional layers can be followed by additional convolutional layers or pooling layers, the fully-connected layer is the final layer. With each layer, the CNN increases in its complexity, identifying greater portions of the image. Earlier layers focus on simple features, such as colors and edges. As the image data progresses through the layers of the CNN, it starts to recognize larger elements or shapes of the object until it finally identifies the intended object.

Convolutional layer

The basic building block for a CNN is the convolution layer and the majority of the computation takes place. It requires a few input data components, a filter, and a map. Suppose the entry is a color picture that consists of a matrix of three-dimensional pixels. The input therefore has three dimensions — one height, width and depth — that are RGB's in a picture. We also have a kernel or a filter, which passes through the reception areas of the picture, verifying whether the feature is present. The detector is also used. It is known as a convergence process.

Pooling Layer

The down sampling layers lead to a reduction in dimensionality, lowering the number of input parameters. The bundling operation swells a filter across the whole input in the same way as the convolution layer, but the distinction is that it has no weight. Instead, the kernel uses an aggregation function to populate the output array for the values in the receiving field. Two major forms of pooling are available:

Max pooling: while the filter is moving over the input it chooses to send the pixel to the output array with the maximum value. In comparison with the average pooling, this method is utilized more often.

Average pooling: When the filter passes through the input, the average value within the receptive area to be sent to the output array is calculated.

Although many information is lost in the pooling layer, the CNN also offers some advantages. It reduces complexity, improves efficiency and reduces the danger of overcasting.

Fully-Connected Layer

The whole layer name expresses itself appropriately. As noted above, the input picture pixel values are not directly linked in partially connected levels to the output layer. However, each node in the output layer is directly linked to a node in the last layer in the completely connected layer.

The classification work of this layer is dependent on the characteristics collected by the preceding layers and their distinct filters. While convolutional and pooling layers employ ReLu functions, FC layers often use a softmax activation function to correctly categorize inputs, which creates a 0 to 1.

3.2 Medical knowledge about brain tumor

A brain tumor is an abnormal brain mass or proliferation of cells.

There are numerous distinct brain tumors. Some brain tumors are not cancerous (benign), others are cancerous. Some brain tumors (malignant). In your brain (primary brain tumors), brain tumors may begin or cancer may start otherwise and spread as secondary (metastatic) brain tumors to your brain.

It can vary widely how fast a brain tumor grows. The growth rate and the location of a brain tumor dictate how it affects your nervous system's function.

Primary brain tumors originate in the brain itself or in tissues close to it, such as in the brain-covering membranes (meninges), cranial nerves, pituitary gland or pineal gland.

Primary brain tumors begin when normal cells develop changes (mutations) in their DNA. A cell's DNA contains the instructions that tell a cell what to do. The mutations tell the cells to grow and divide rapidly and to continue living when healthy cells would die. The result is a mass of abnormal cells, which forms a tumor.

In adults, primary brain tumors are much less common than are secondary brain tumors, in which cancer begins elsewhere and spreads to the brain.

4. Proposed system

4.1 Introduction

The main idea of the project is to use the machine learning knowledge to solve the brain tumor problems and detect it to make it easy for the specialists to give the patient the perfect treatment according to its condition, by using the CNN to detect the tumor from MRI images and the main phases of our project is preprocessing (in this phase we enhance and prepare the dataset to be used in the next phases), training the model (in this phase we use the dataset to train the model how to detect the tumor from MRI images to give the tumor place in the brain) and prediction (this phase is the test phase for the project, we take a MRI image and give it to the program and if there is a tumor the program should detect the place of it) and this figures and flowcharts show each phase of the project :

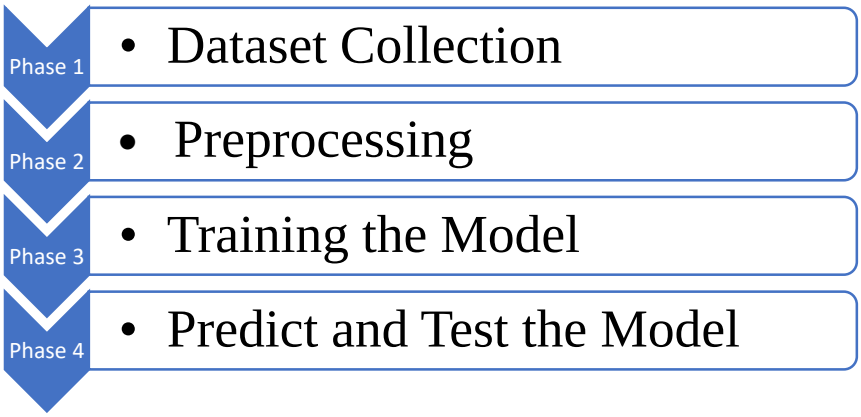

f***ig.8*** *show the flow of the model.*

In this application we have built two different models, and they depend on CNN in their construction, and in this chapter, we will review a detailed explanation of the two models used and also, we will deal with a detailed explanation of the dataset used in this application and how to use it in the application and also, we will deal with explanation of the code through the flowchart. We show the stages that the dataset goes through in detailed points such as preprocessing, training and prediction.

4.2 Dataset Collection:

Dataset description

Since BraTS'16, data sets utilized for the challenges of this year have been upgraded by professional board-certified neurodiologists, including more routine multimodal 3T MRI images and all ground-truth labelling.

The training, validation and testing data on the BraTS challenge for this year will provide ample multi-institutional clinically acquired pre-operational glioblastoma MRI (GBM/HGG) and lower glioma (LGG) multi-institutional scan with pathologically confirmed diagnosis and available operational system.

The challenge training dataset BraTS 2017 comprises of 210 MRI preoperative scans from HGG subjects and 75 LGG subject images, while the 2018 challenge validation dataset BraTS has 66 different 3D-MRI multimodality scans.

Images from 19 distinct facilities were gathered from various suppliers using the MR scanners and 3T field strength.

They include co-registered MRI native (T1) and T1-weighted (T1Gd) contrasts as well as MRI co-registered T2 and MRI (FLAIR) attensified fluid (T2).

All BraTS'2017 3D-MRI data sets are 240 per 240 per 155.

They are distributed, co-registered and interpolated to the same anatomical template (1 mm3).

All RMI volumes were manually segmented by one to four raters, with expert neuro-radiologists having confirmed their annotations. The edema, necrosis and non-simulating tumors and active/improving tumors each were segmented.

4.3 preprocessing phase (used in two models that we are use it):

Preprocessing Decryption:

First, a minimal pre-processing of MRI data is applied, as in [7]. The 1% highest and lowest intensities were removed, then each modality of MR images was normalized by subtracting the mean and dividing by the standard deviation of the intensities within the slice. To address the class imbalance problem in the data, data augmentation technique [6] were employed. This consists in adding new synthetic images by performing operations and transformations on data and the

corresponding manual tumors segmentation images obtained by human experts (ground truth data). The transformations comprise rotation, translation, and horizontal flipping and mirroring.

Preprocessing Flowchart:

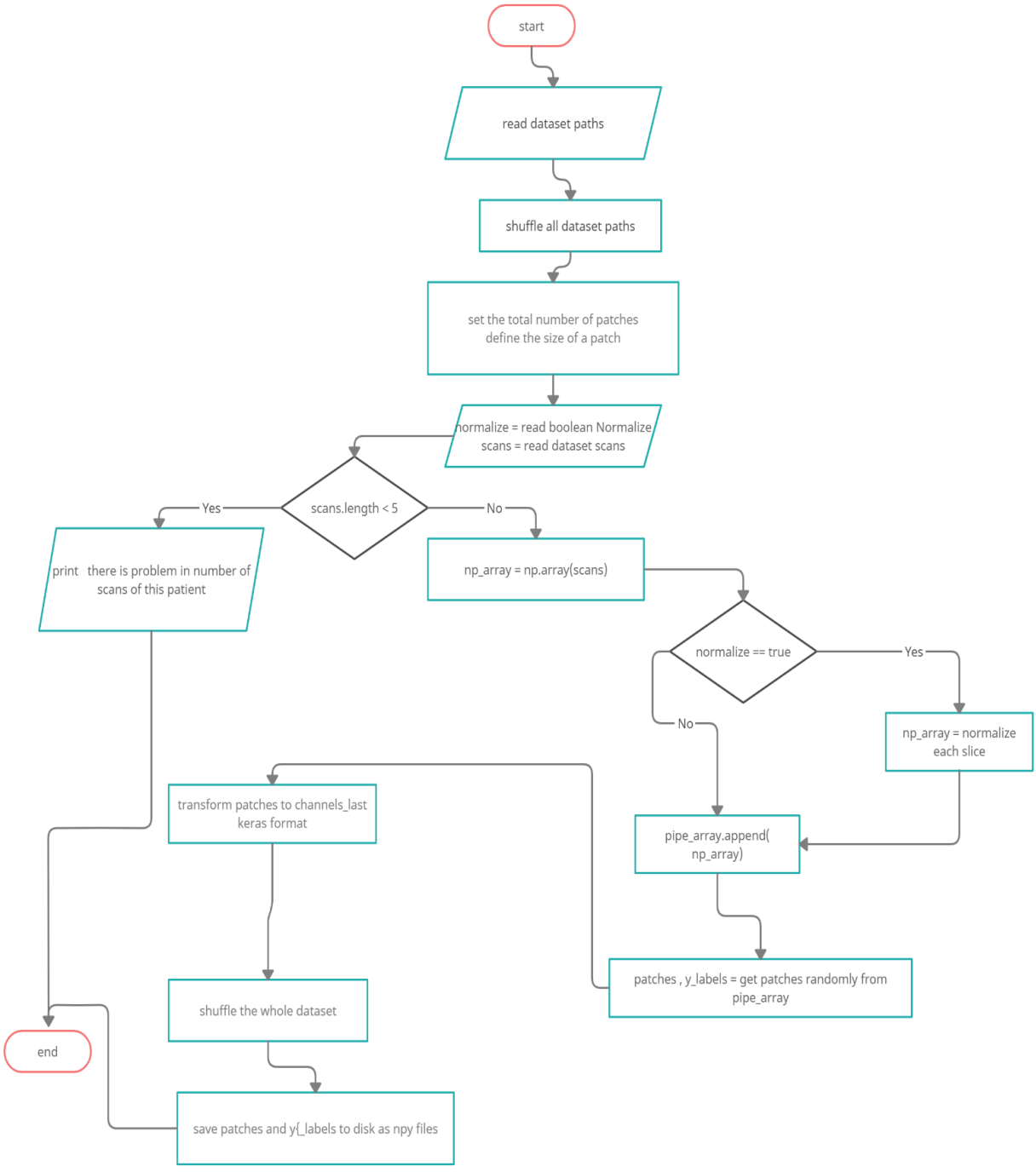

fig.9 *show the preprocessing flowchart*

4.4 Training phase (Different in two models that we are use it):

4.4.1 U-net brain segmentation based model Architecture and Training

The CNN used in this study has a similar architecture as that of U-net [1]. Our network architecture can be seen in Fig. 3. It consists of a contracting path (left side) and an expanding path (right side). The contracting path consists of 3 pre-activated residual blocks, as in [2, 3], instead of plain blocks in the original U-net. Each block has two convolution units each of which comprises a Batch Normalization (BN) layer, an activation function, called Parametric Rectified Linear Unit (PReLU) [4],instead of ReLU function used in the original architecture [1], and a convolutional layer, like in [5], instead of using Maxpooling [1], with Padding = 2, Stride = 1 and a 3 x 3 size filter. For down sampling, a convolution layer with a 2 x 2 filter and a stride of 2 is applied. At each down sampling step, the number of feature channels is doubled. The contracting path is followed by a fourth residual unit that acts as a bridge to connect both paths. In the same way, the expanding path is built using 3 residual blocks. Prior to each block, there is an upsampling operation which increases the feature map size by 2, followed by a 2 x 2 convolution and a concatenation with the feature maps corresponding to the contracting path. In the last layer of the expanding path, a 1 x 1 convolution with the Softmax activation function is used to map the multi-channel feature maps to the desired number of classes. In total, the proposed network model contains 7 residual blocks, 25 convolution layers, 15 layers of BN and 10159748 parameters to optimize. The designed network was trained with axial slices extracted from training MRI set, including HGG and LGG cases, and the corresponding ground truth segmentations. The goal is to find the network parameters (weights and biases) that minimize a loss function. In this work, this can be achieved by using Stochastic Gradient Descent algorithm (SGD) [6], at each iteration SGD updates the parameters towards the opposite direction of the gradients. In our network model, we used a loss function categorical crossentropy because it’s the loss function that benefit with our dataset.

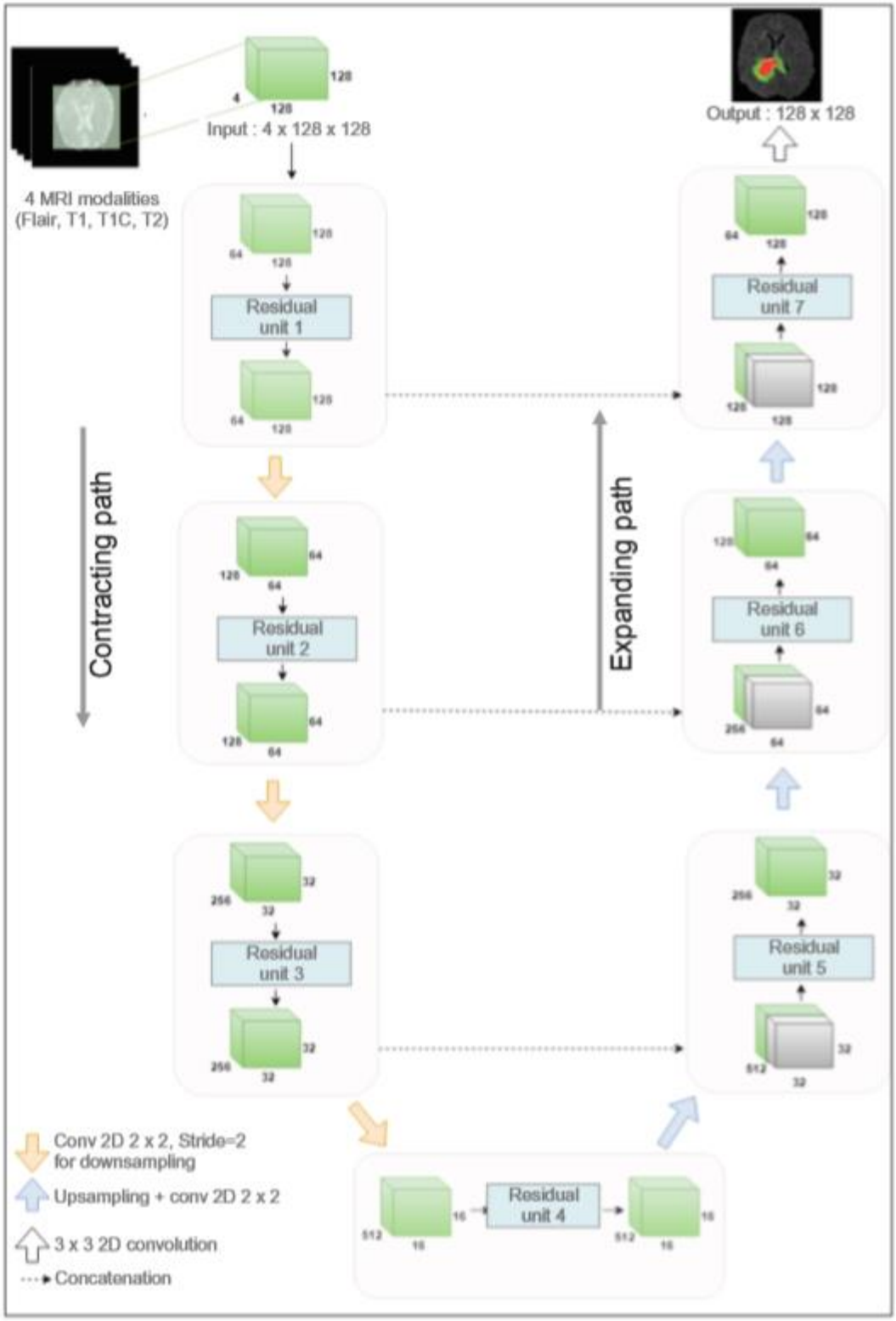

fig. 10. *Architecture of the proposed Deep Convolutional Neural Network*.

- Model training phase flowchart:

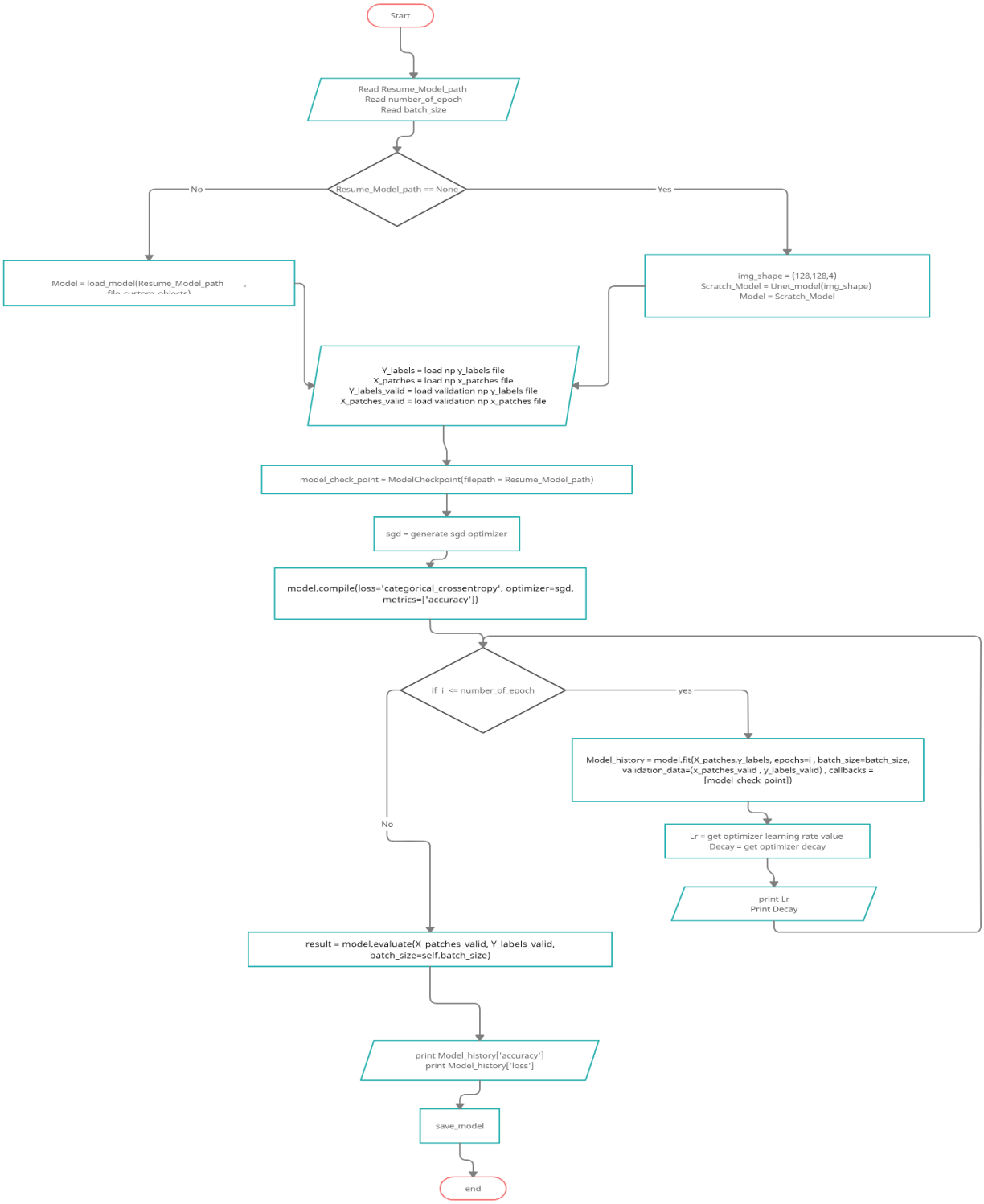

fig.11 *Show the training flowchart*

4.4.2 Convent brain segmentation based model Architecture and Training

The ConvNet architecture, used for slice wise segmentation along each plane, is an encoder-decoder type of network. The encoder or the contracting path uses pooling layers to down sample an image into a set of high-level features, followed by a decoder or an expanding part which uses the feature information to construct a pixel-wise segmentation mask. The main problem with this type of networks is that, during the down sampling or the pooling operation the network loses spatial information. Up sampling in the decoder network then tries to approximate this through interpolation. This produces segmentation error around the boundary of the region-of-interest (ROI) or volume-of-interest (VOI). It is a major drawback in medical image segmentation, where accurate delineation is of utmost importance.

We also incorporate shortcut connections to copy and concatenate the receptive fields (after convolution block) from the encoder to the decoder part, in order to help the decoder network localize and recover the object details more effectively. These connections allow the network to simultaneously incorporate high-level features with the pixel-level details. The entire segmentation model architecture is depicted in Fig.12.

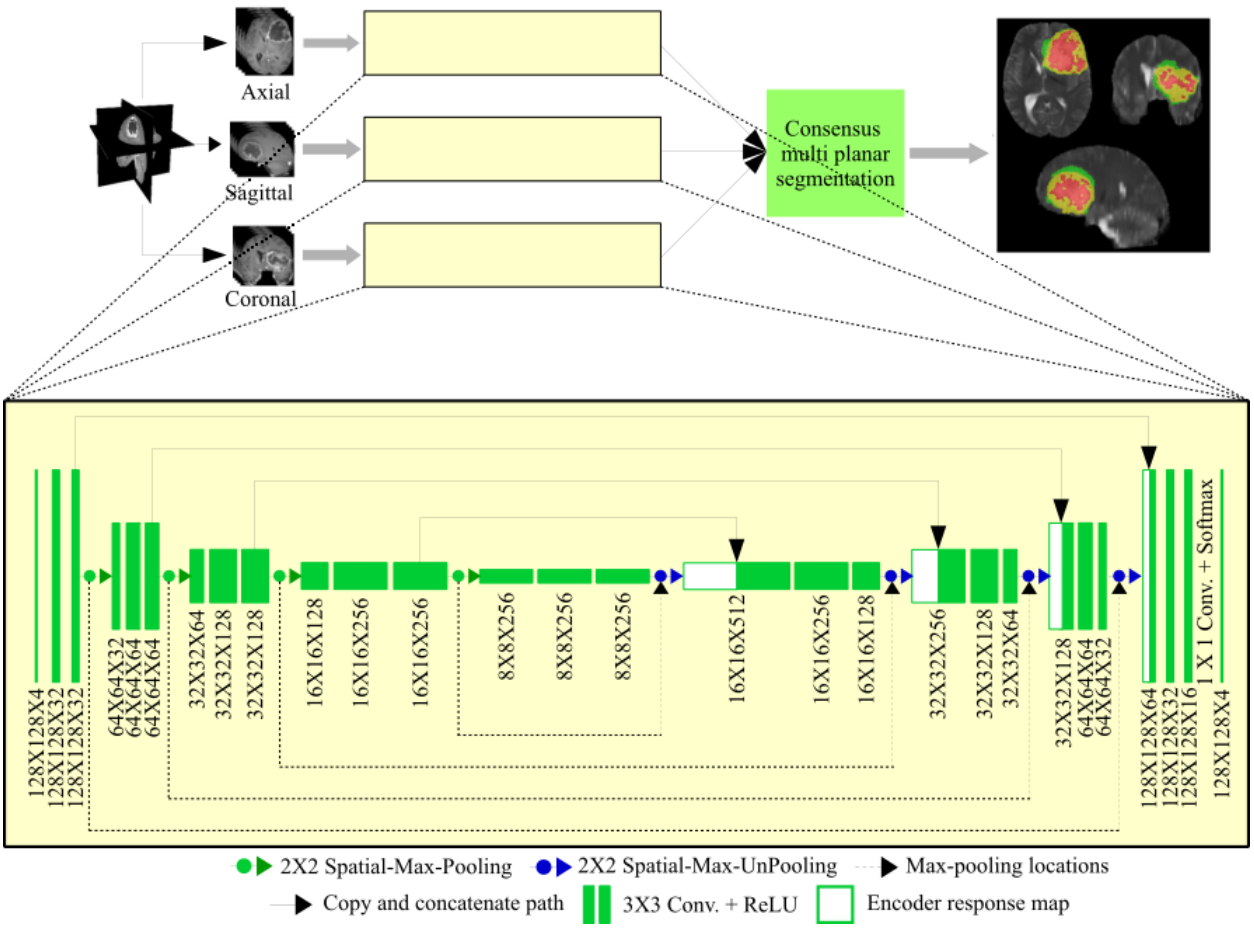

fig.12 *Multi-planar ConvNet architecture for segmentation.*

Each ConvNet is trained on patches of size 128×128×4, extracted from all four MRI sequences corresponding to a particular plane. A randomized patch extraction algorithm, developed by us, is employed. The patch selection is done using an entropy-based criterion. The three ConvNets (along the three planes) are trained end-to-end/pixel-to-pixel, based on the patches extracted from the corresponding ground truth images.

- **Model training phase flowchart:**

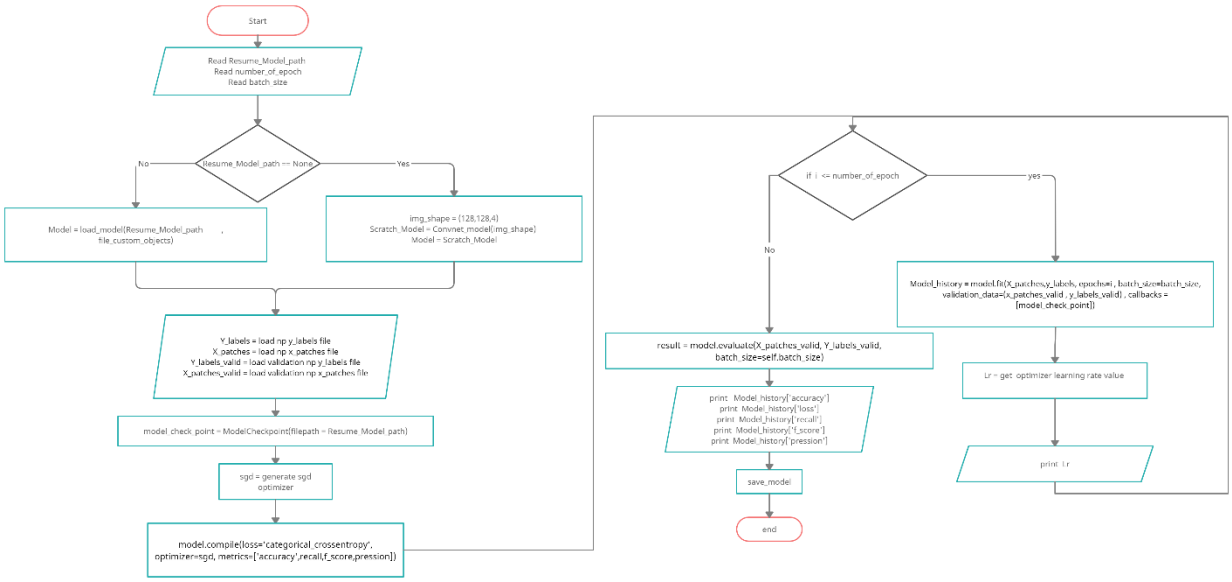

fig. 13. *Show the Model 2 flowchart.*

4.5 Prediction phase (used in two models that we are use it):

After network training, prediction may be performed. This step consists to provide the network with the four MRI modalities of an unsegmented volume that it has never processed or encountered before, and it must be able to return a segmented image to understand prediction code sequence look Fig.14.

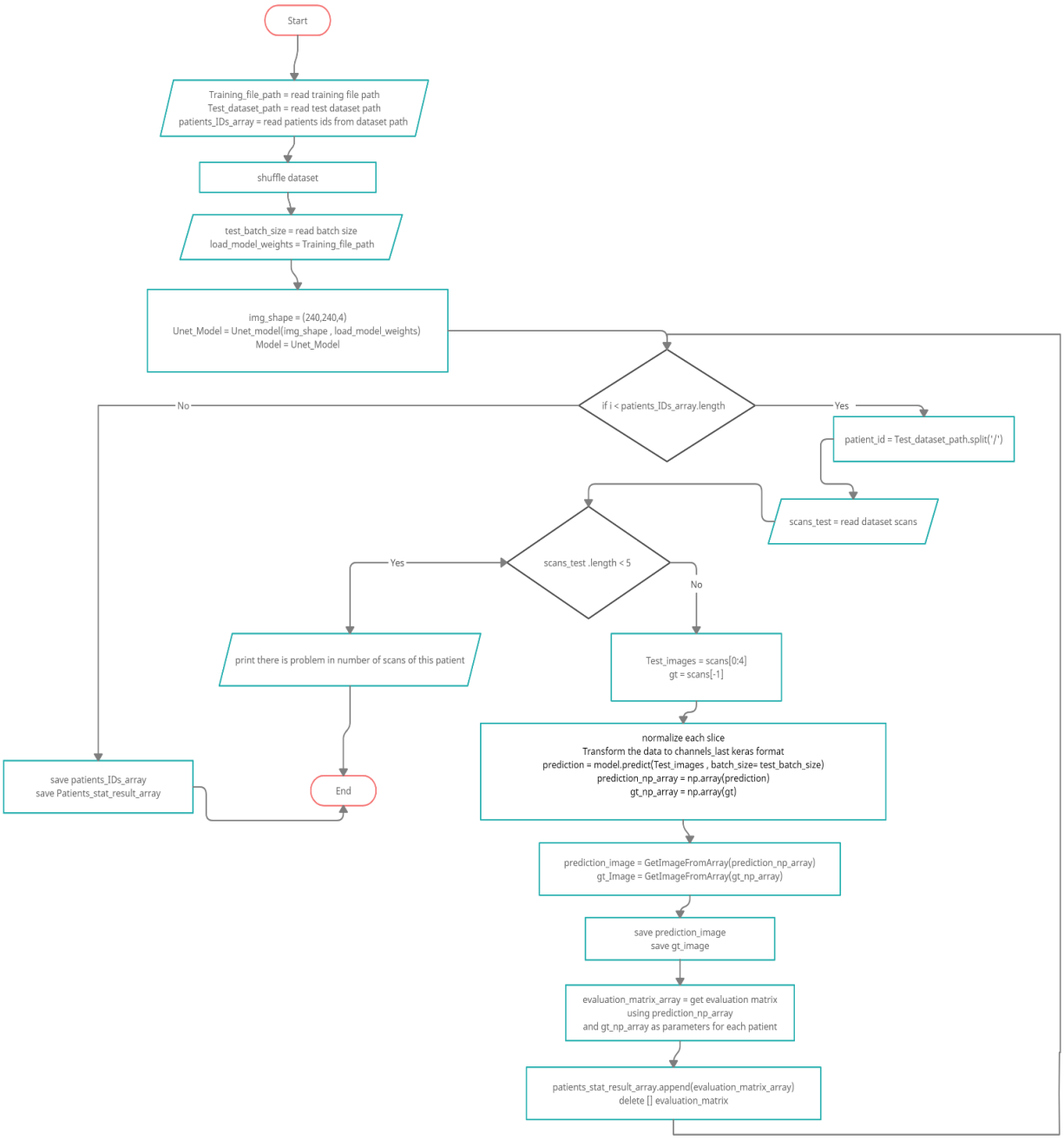

fig. 14. *Show the prediction flowchart*

5. Result Analysis

In this chapter we will present the result of our project for the two models and these two models is deferent architectures for the CNN network for the brain tumor detection problem based in different datasets like BRT's 2017 and BRT's 2018.

5.1- segmentation result

5.1.1- U-net brain segmentation based model

Does the segmentation for the brain tumor as we learn from the previous chapter and give the following results in case of the patient was a HGG or LGG type:

The HGG type from the coronal view for the brain:

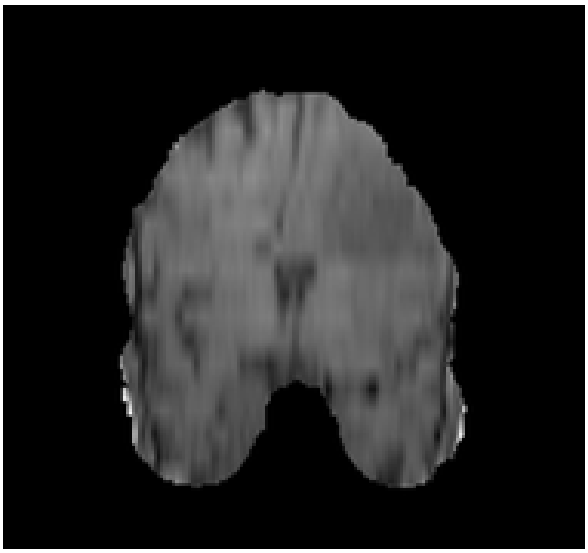

fig.15 shows the t1 coronal view.

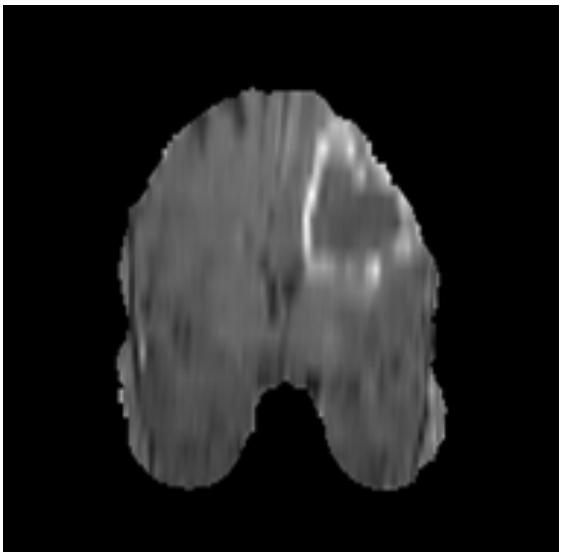

fig.16 shows the t1c coronal view

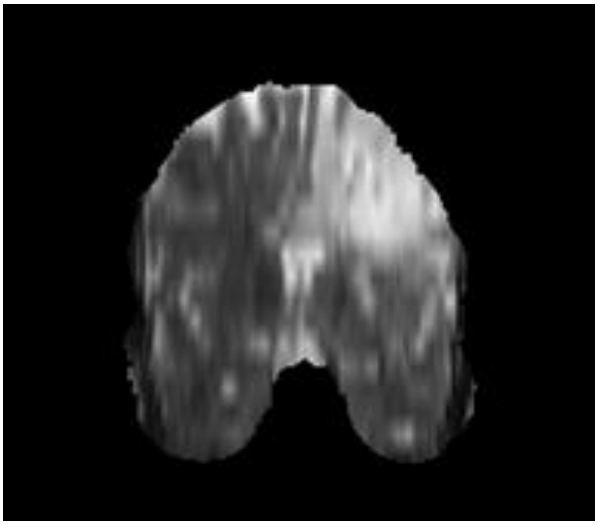

fig.17 shows the t2 coronal view

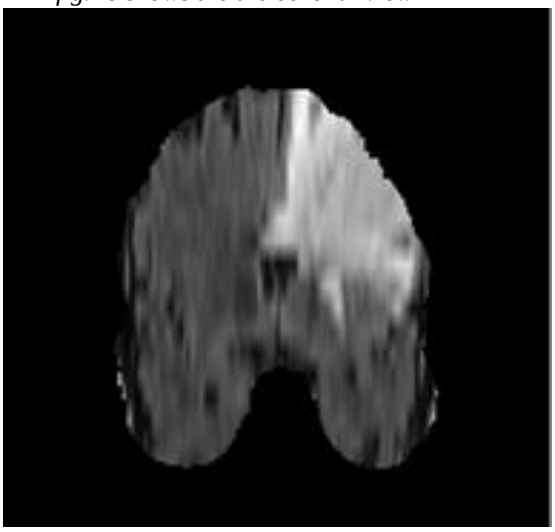

fig.18 shows the flair coronal view

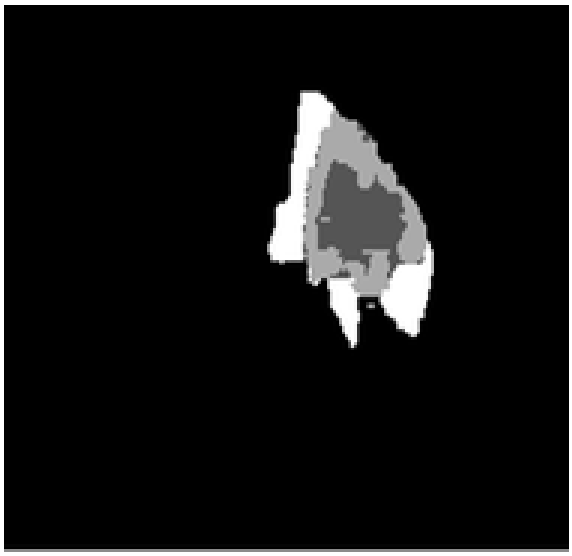

fig.19 shows the ground truth coronal view

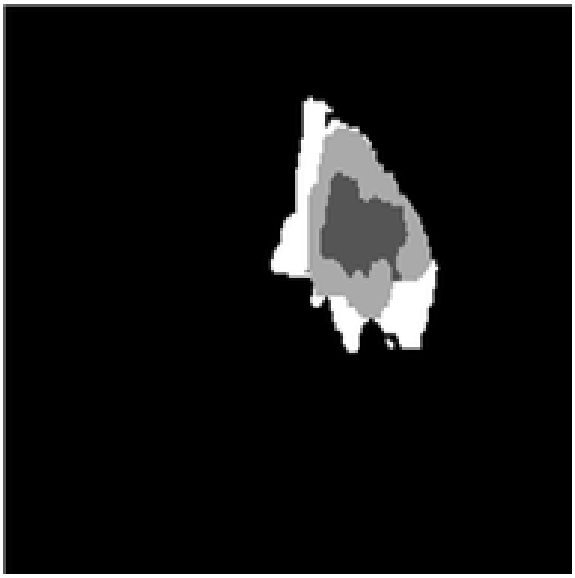

fig.20 shows the prediction coronal view

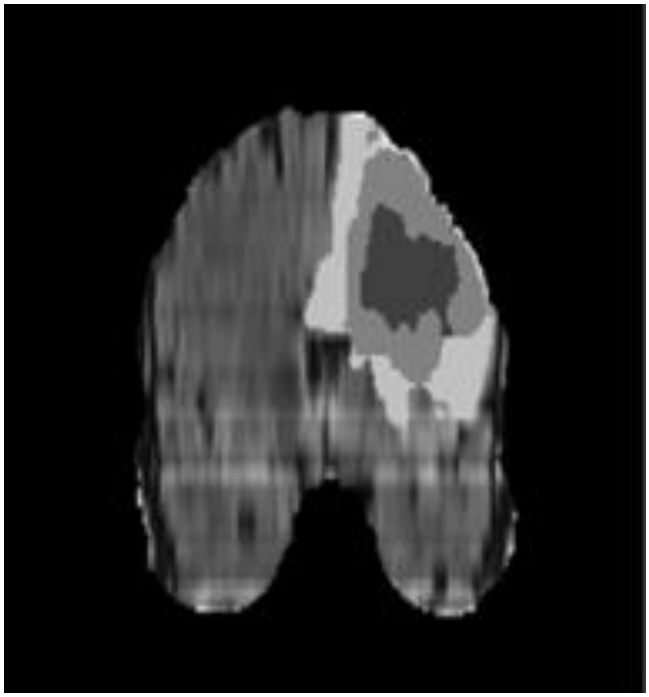

fig.21 shows the final GUI prediction coronal view

the results for the sagittal view for the HGG patient:

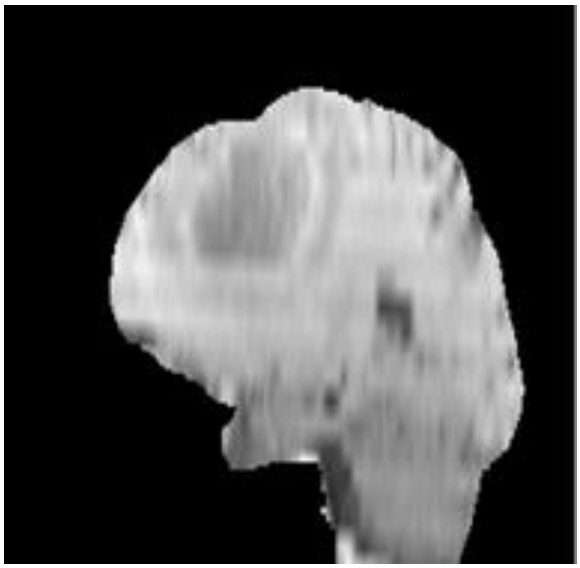

fig22. shows the t1 sagittal view

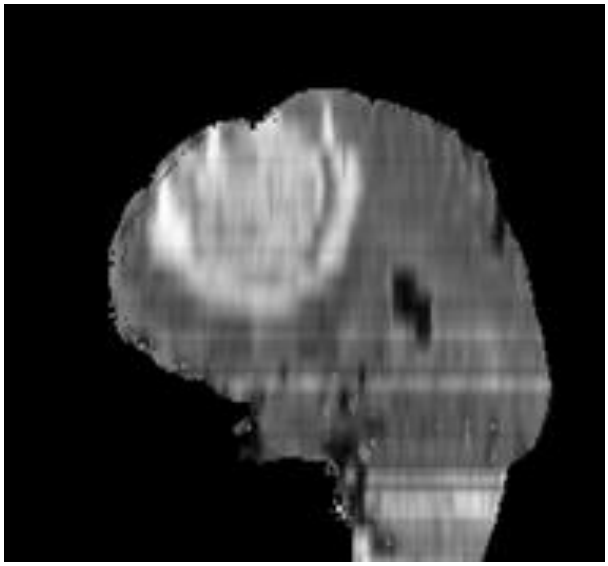

fig.23 shows the t1c sagittal view

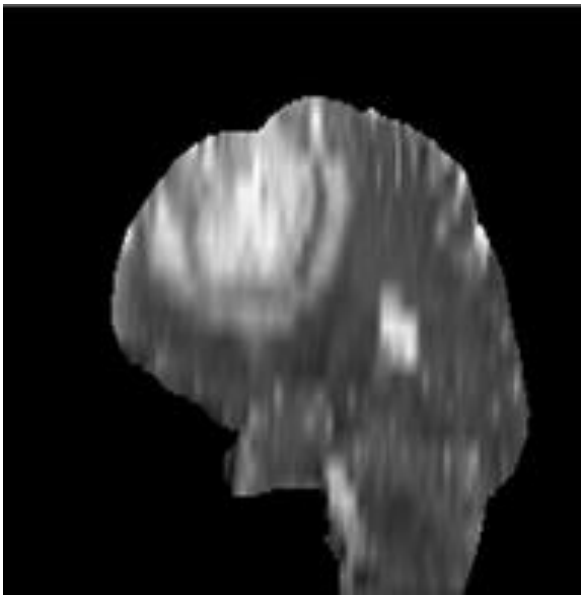

fig.24 shows the t2 sagittal view

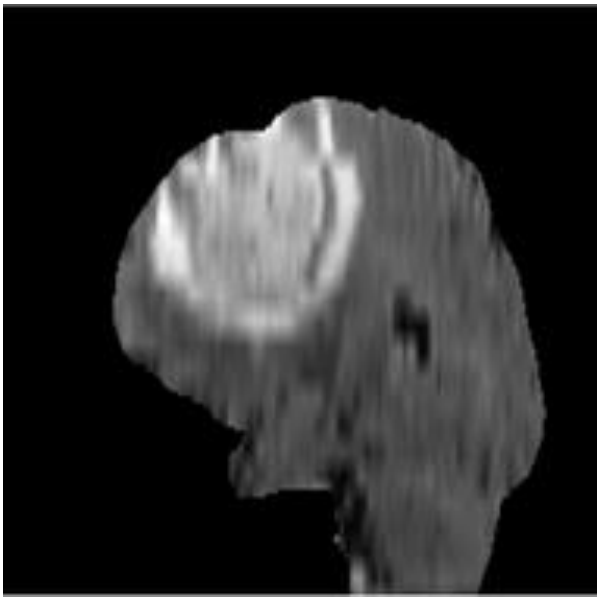

fig.25 shows the flair sagittal view

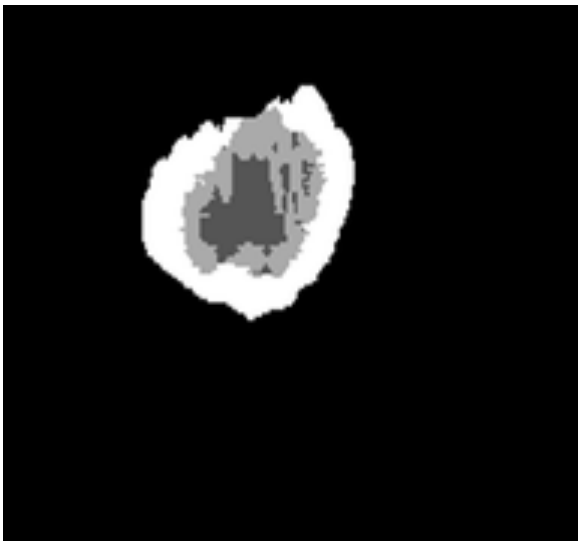

fig.26 shows the ground truth sagittal view

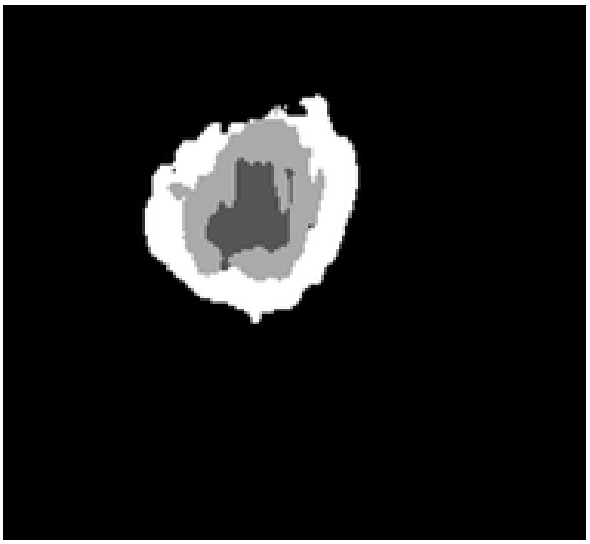

fig.27 shows the prediction sagittal view

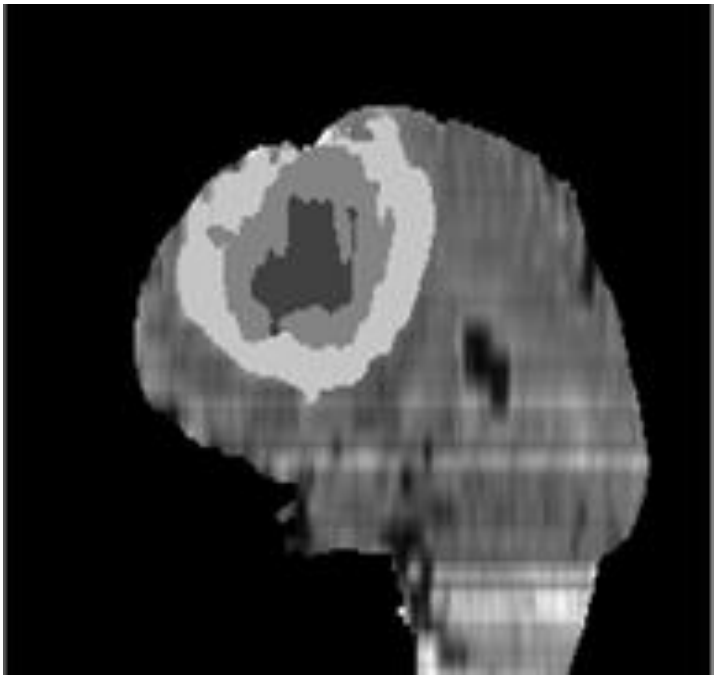

fig.28 shows the final GUI prediction sagittal view

The axial view for the brain in HGG patient:

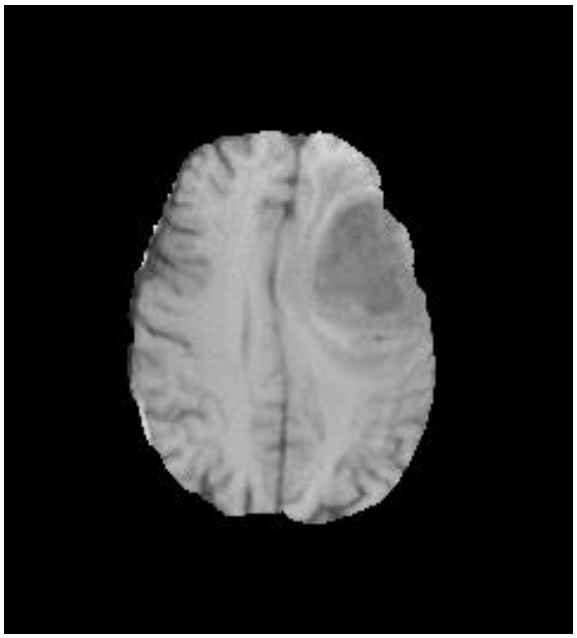

fig.29 shows the t1 axial view

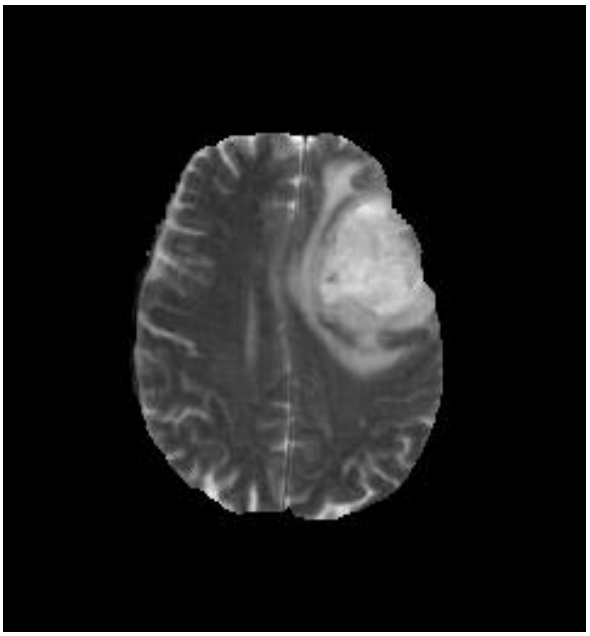

fig.30 shows the t2 axial view

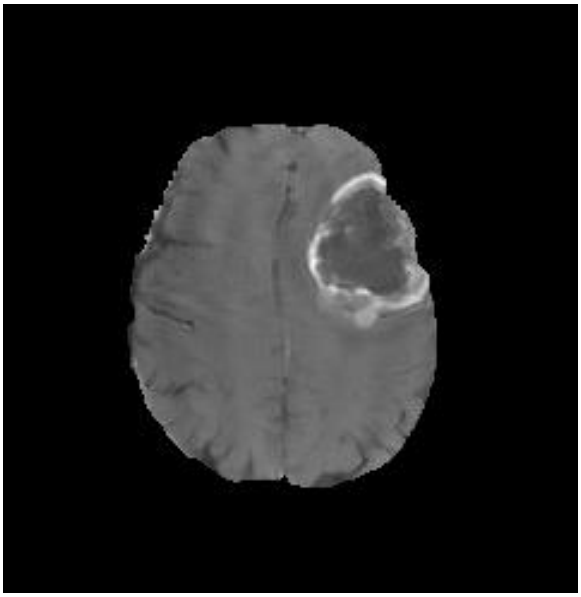

fig.31 shows the t1c axial view

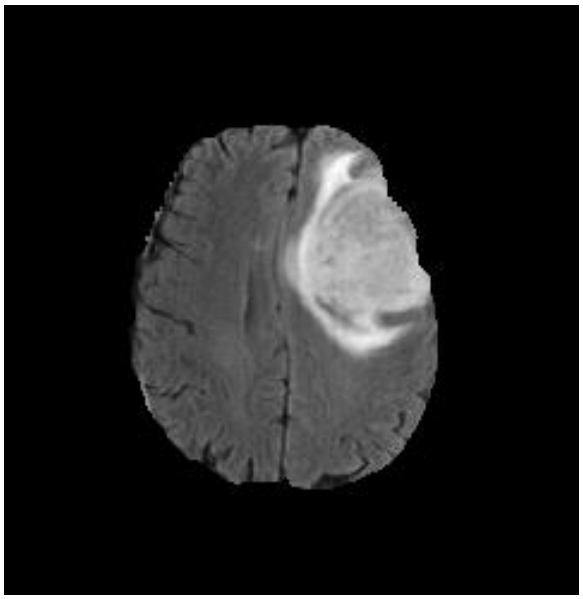

fig.32 shows the flair axial view

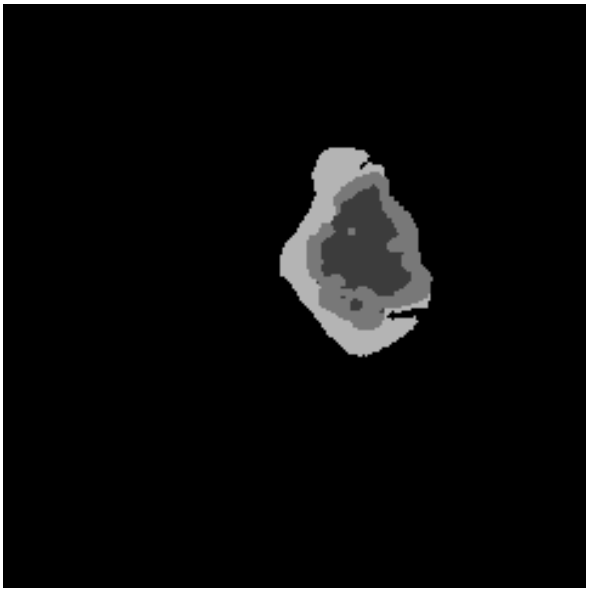

fig.33 shows the ground truth axial view

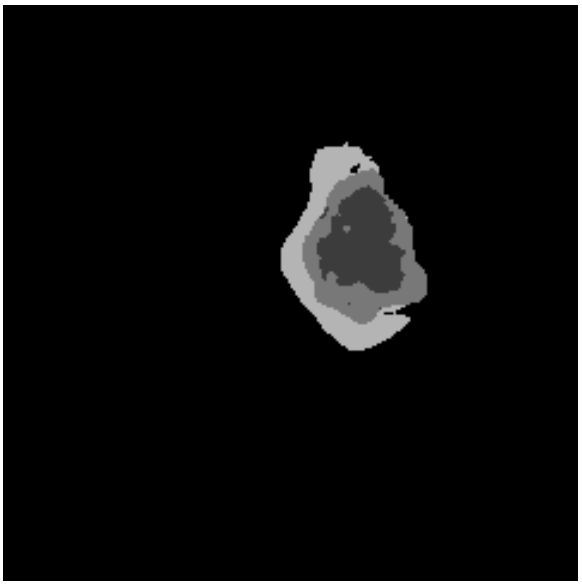

fig.34 shows the prediction axial view

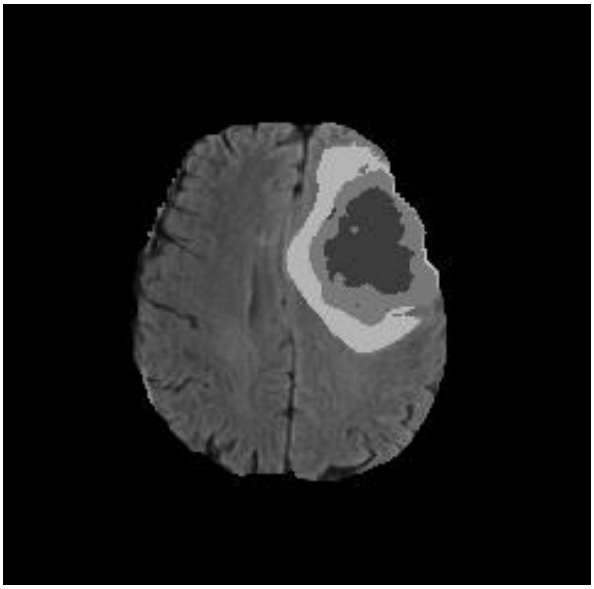

fig.35 shows the final GUI prediction axial view

The coronal view for the LGG patient:

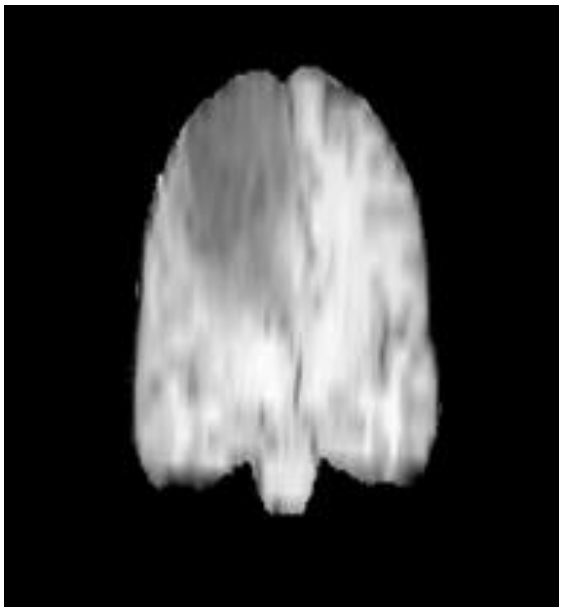

fig.36 shows the t1 coronal view

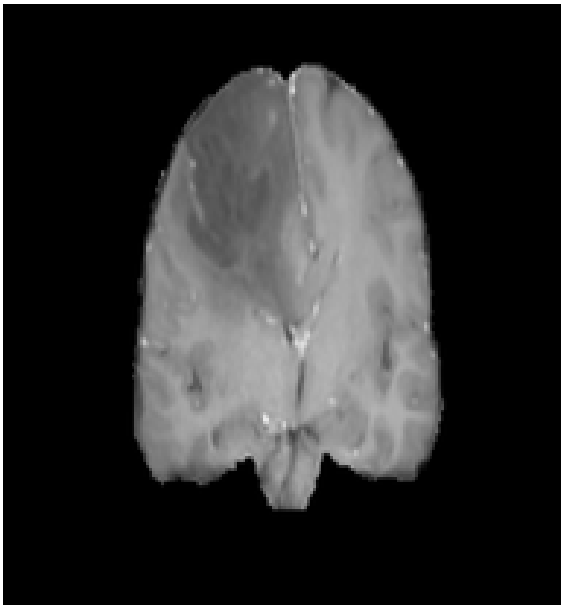

fig.37 shows the t1c coronal view

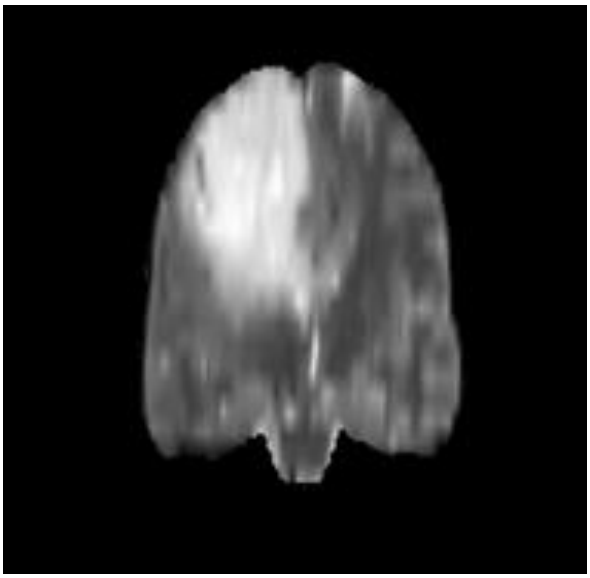

fig.38 shows the t2 coronal view

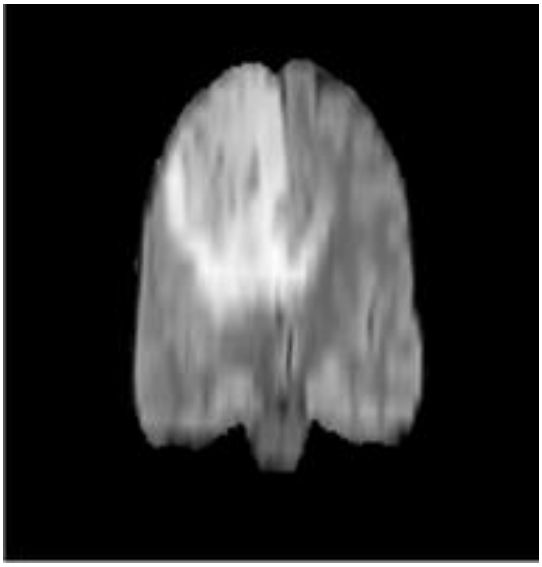

fig.39 shows the flair coronal view

fig.40 shows the ground truth coronal view

fig.41 shows the prediction coronal view

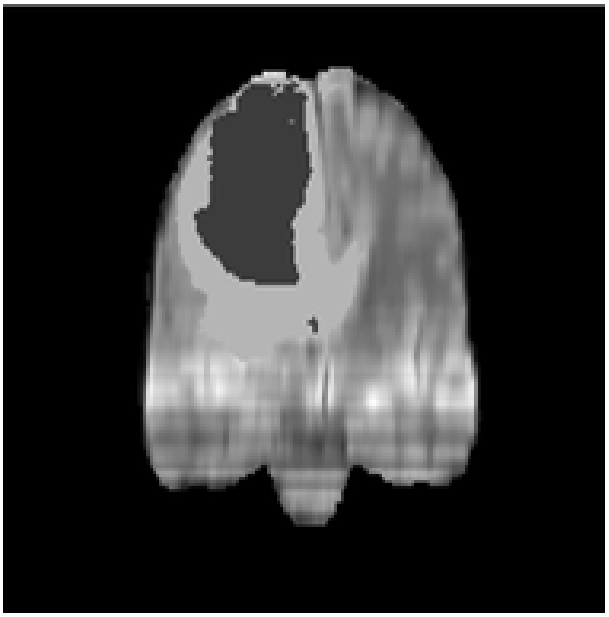

fig.42 show the final GUI prediction Coronal view

the sagittal view of LGG patient

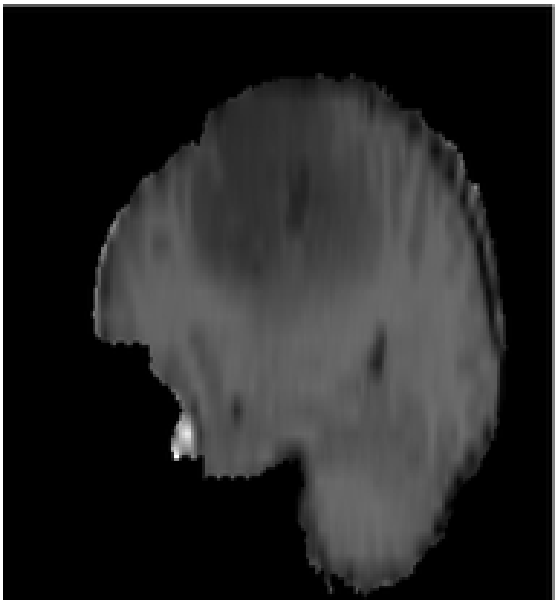

fig.43 shows the t1 sagittal view

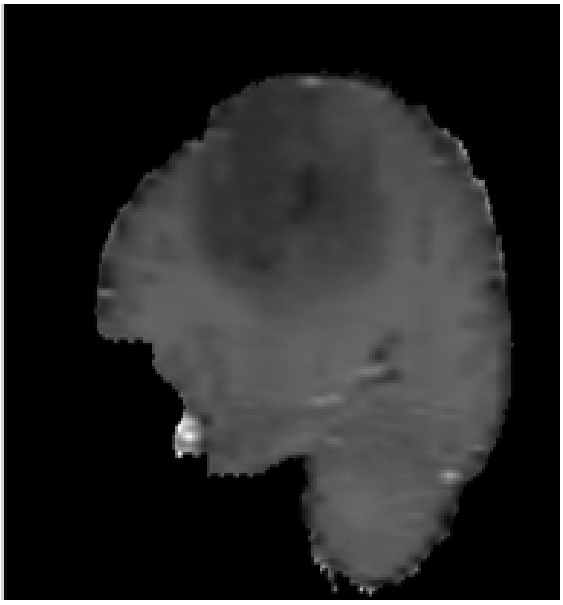

fig.44 shows the t1c sagittal view

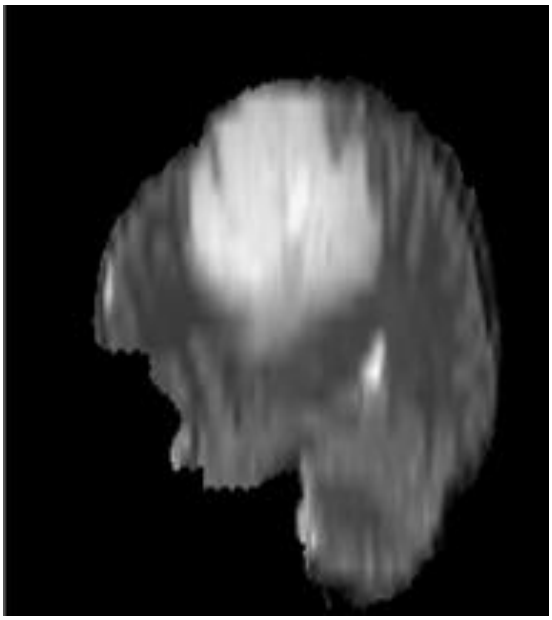

fig.45 shows the t2 sagittal view

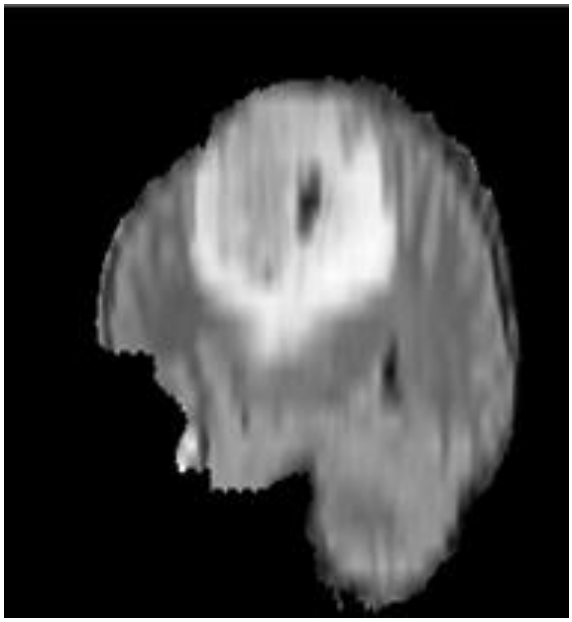

fig.46 shows the flair sagittal view

fig.47 shows the ground truth sagittal view

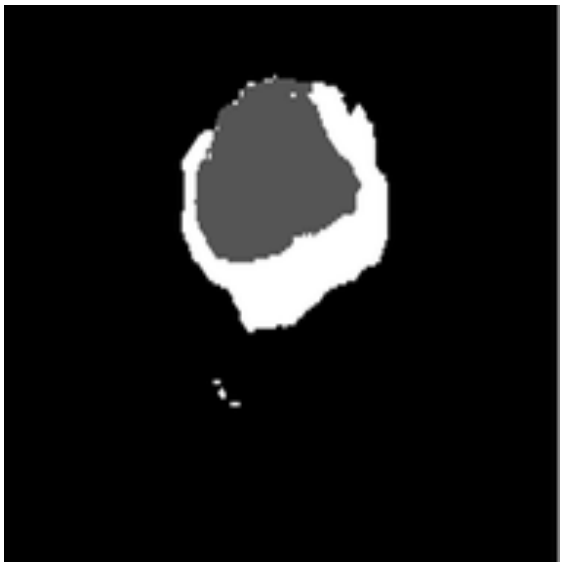

fig.48 shows the prediction sagittal view

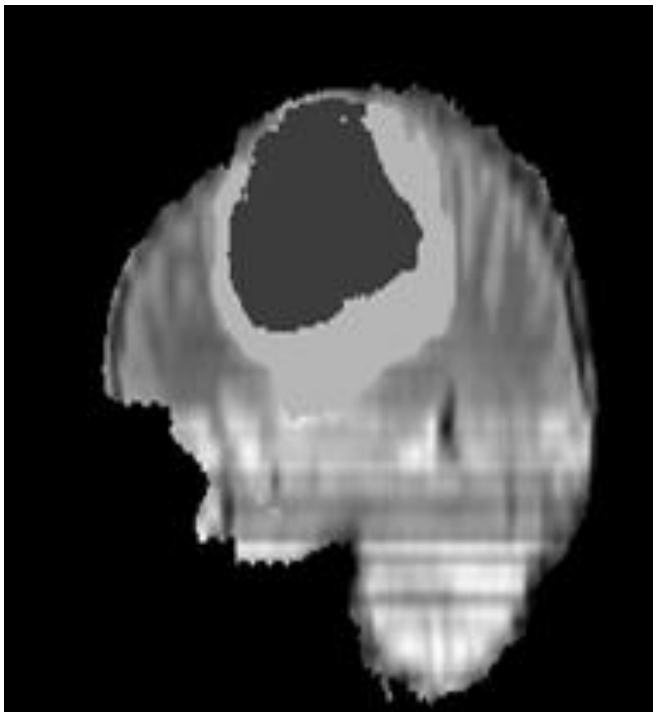

fig.49 shows the final GUI prediction sagittal view

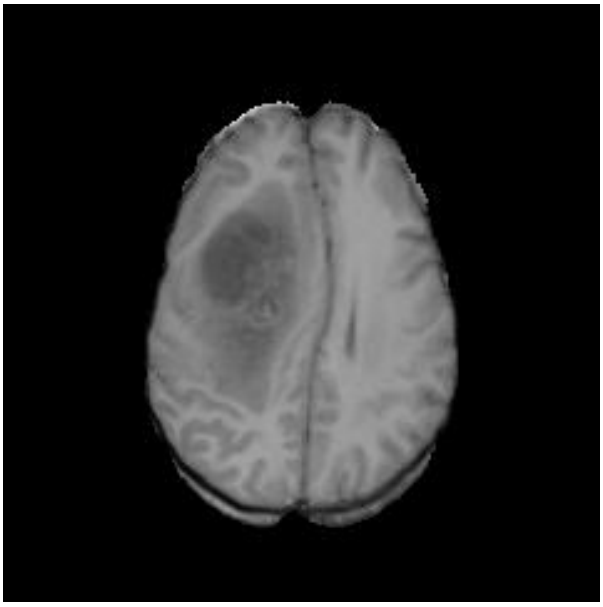

fig.50 shows the t1 sagittal view

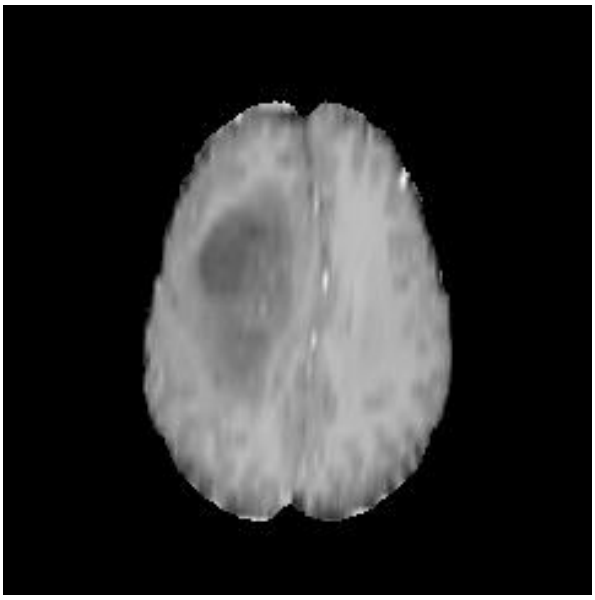

fig.51 shows the t1c sagittal view

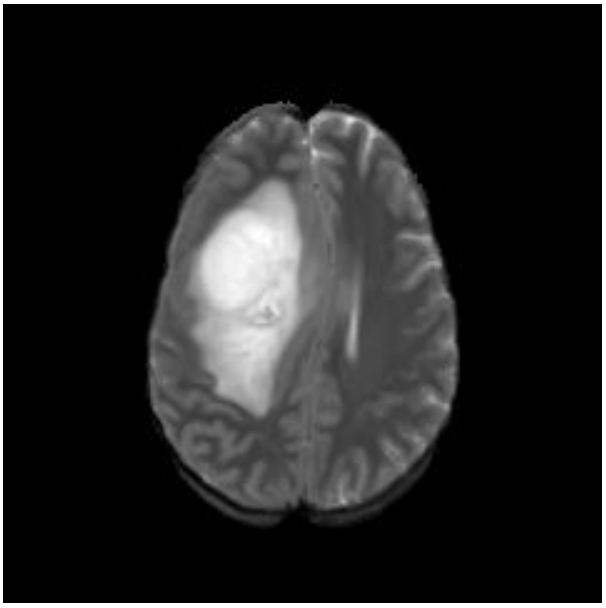

fig.52 shows the t2 sagittal view

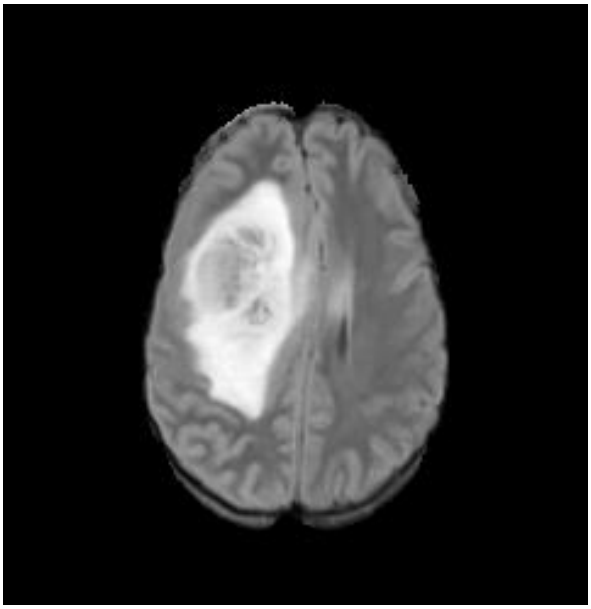

fig.53 shows the flair sagittal view

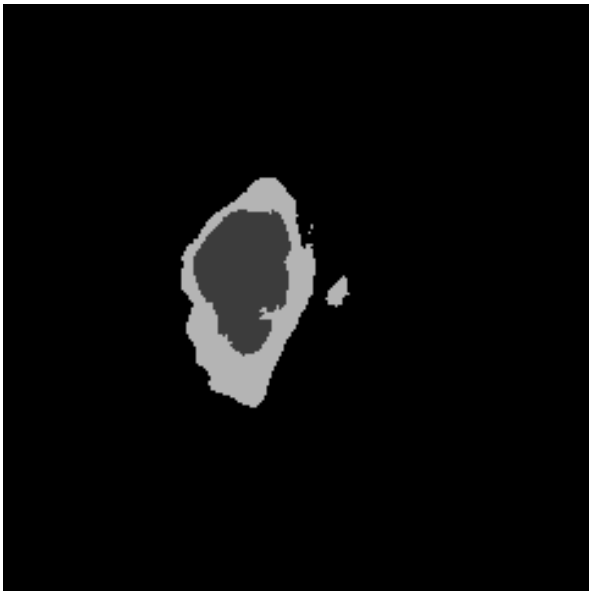

fig.54 shows the ground truth sagittal view

fig.55 shows the prediction sagittal view

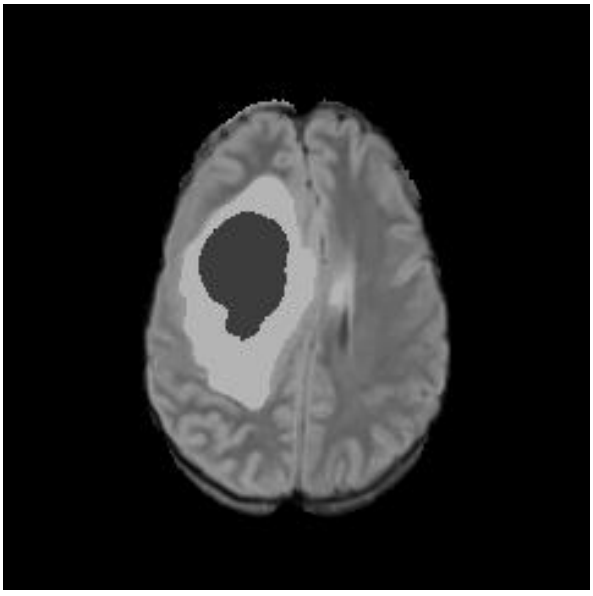

fig.56 shows the final GUI prediction sagittal view

U-net brain segmentation based model graphs and results:

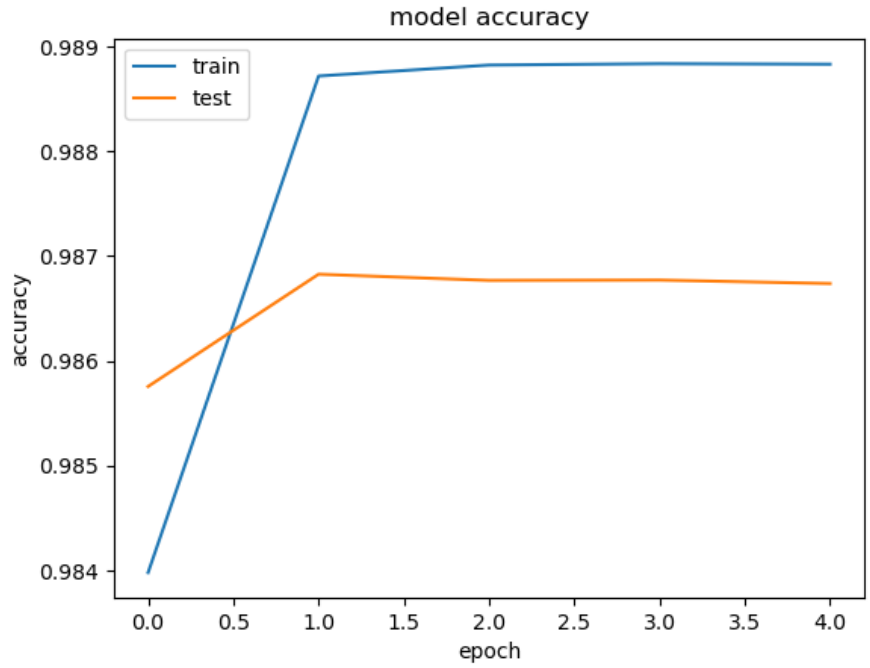

fig.57 shows the accuracy of the first model.

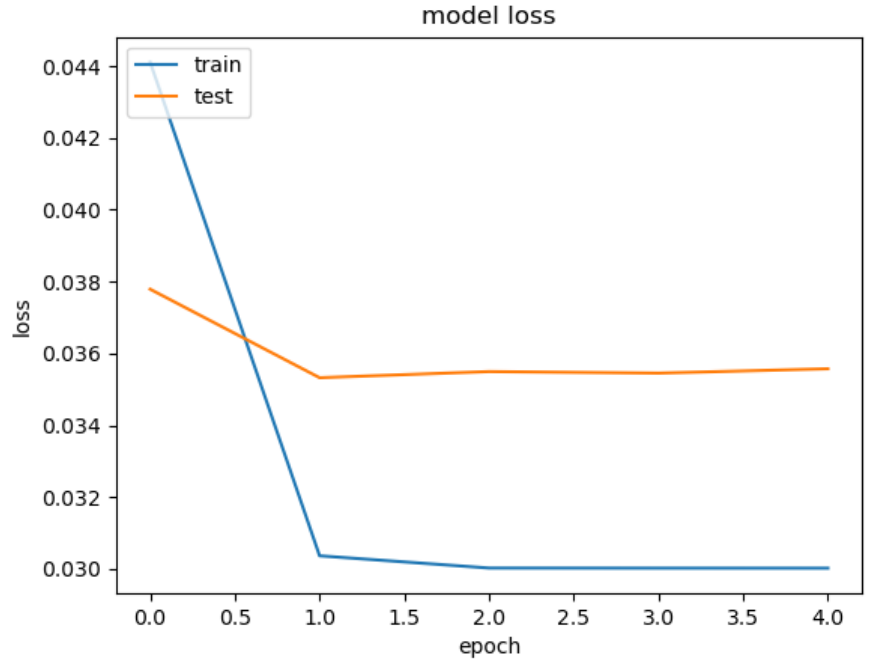

fig.58 shows the loss of the first model.

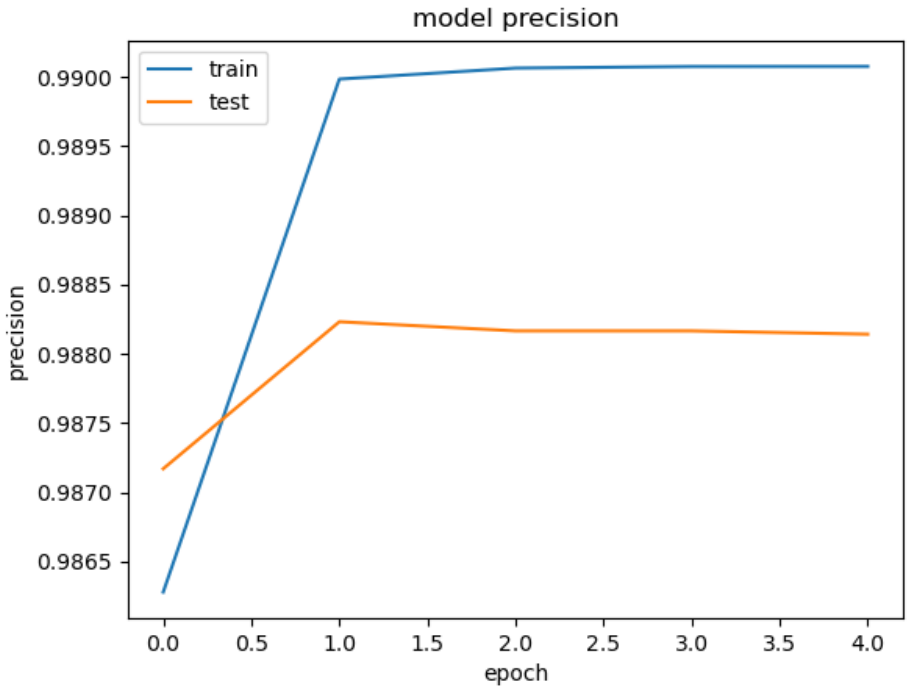

fig.59 shows the precision of the first model.

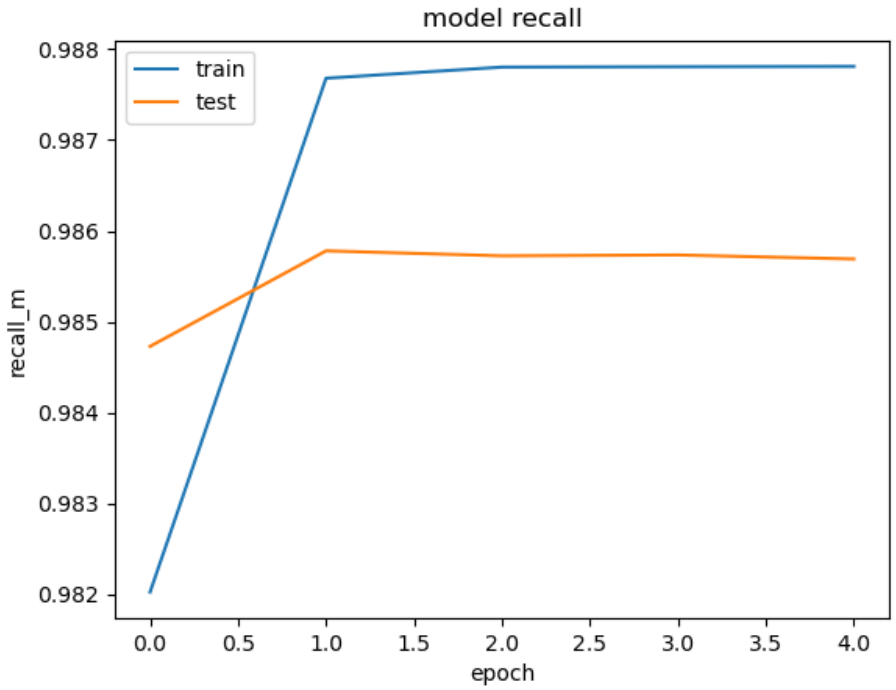

fig.60 show the recall of the first model

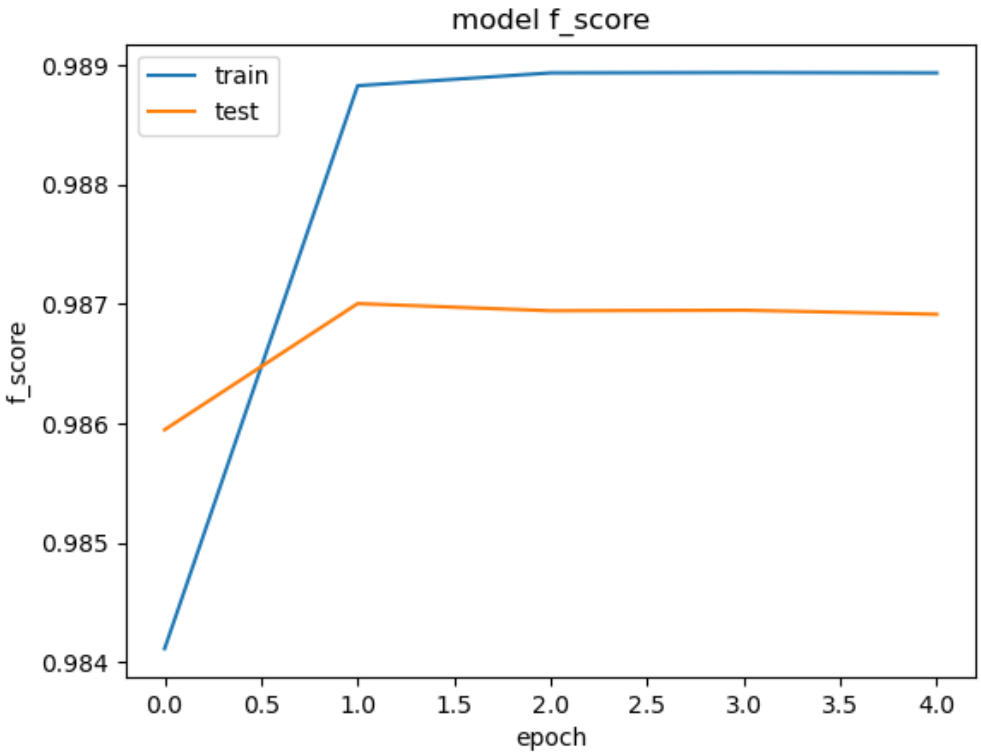

fig.61 shows the f_score of the first model.

5.1.2- convent brain segmentation based model

Does the segmentation of the brain tumor based on the CNN but in a different architecture from the first model with the following result:

The HGG results of segmentation:

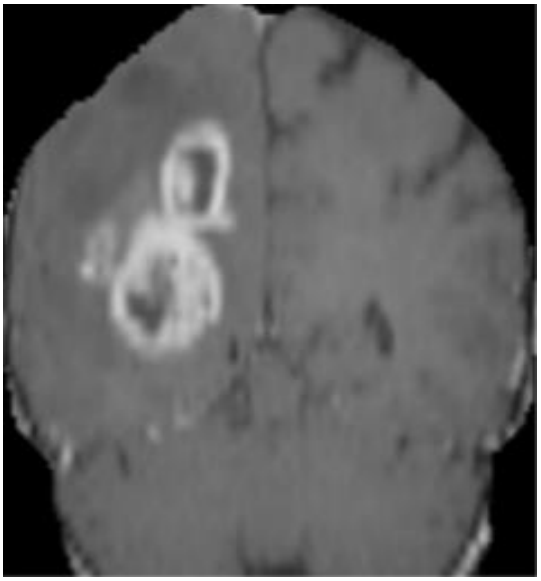

fig.62 shows the flair coronal view

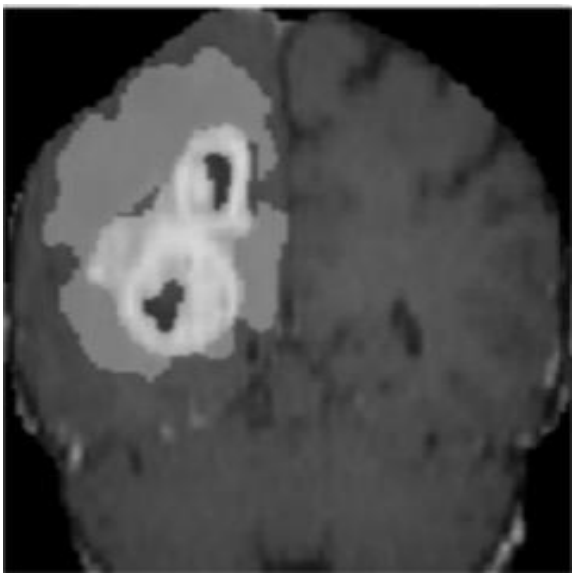

fig.63 shows the prediction coronal view

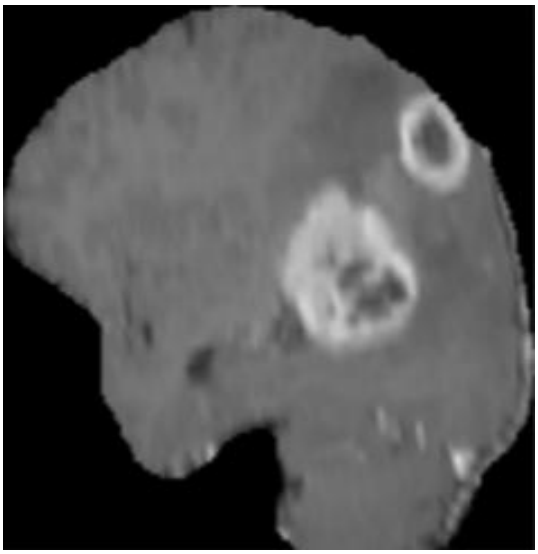

fig.64 shows the flair sagittal view

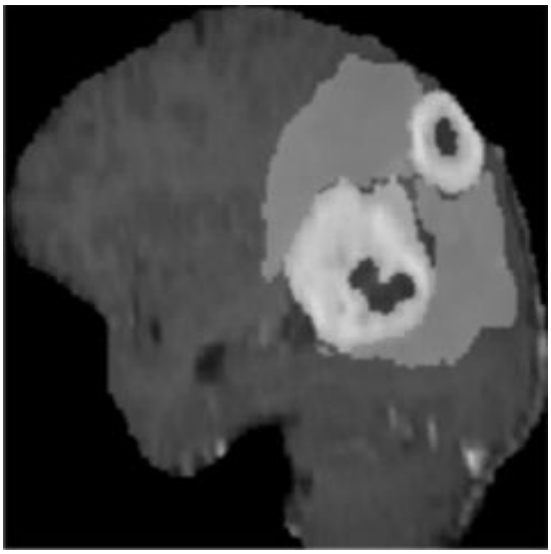

fig.65 shows the prediction sagittal view

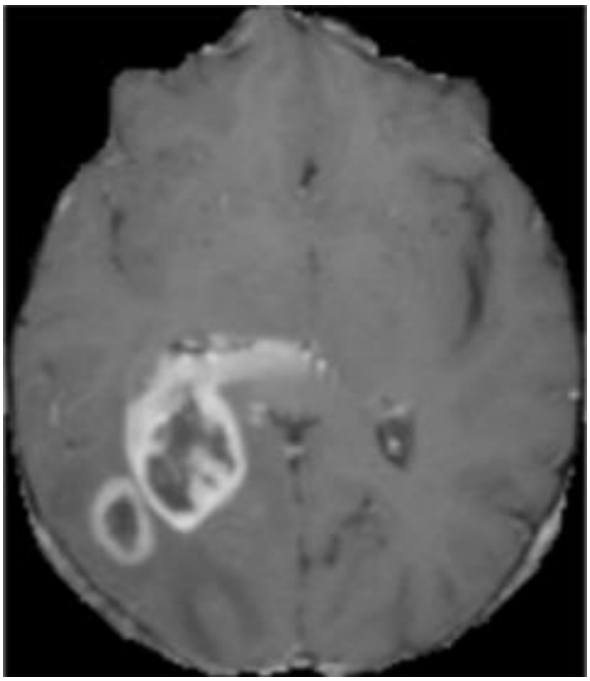

fig.66 shows the flair axial view

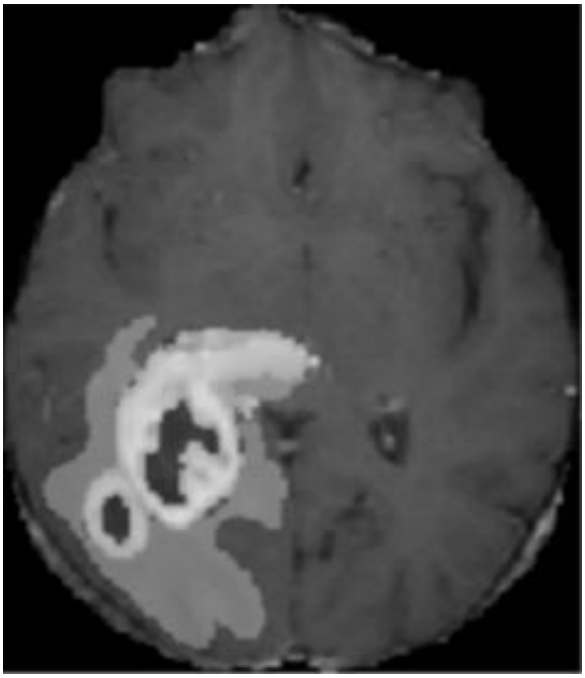

fig.67 shows the prediction axial view

the LGG results of segmentation:

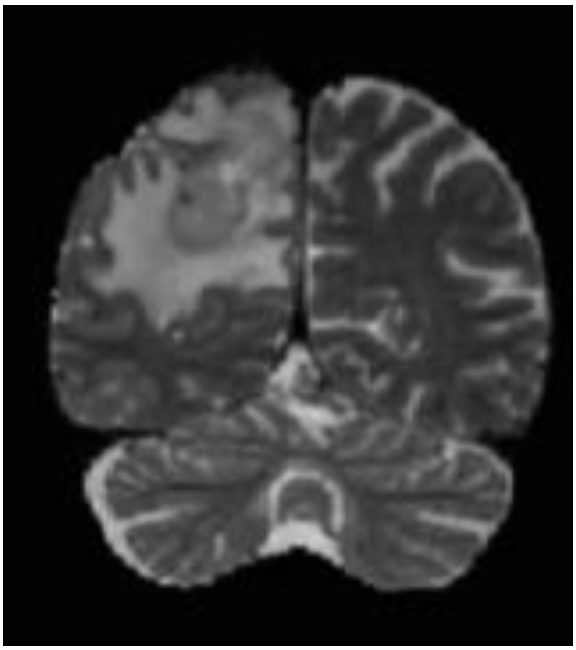

fig.68 shows the flair coronal view

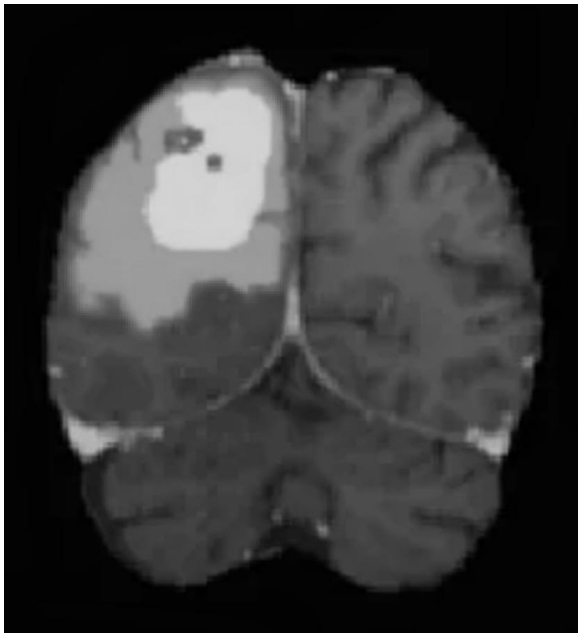

fig.69 shows the prediction coronal view

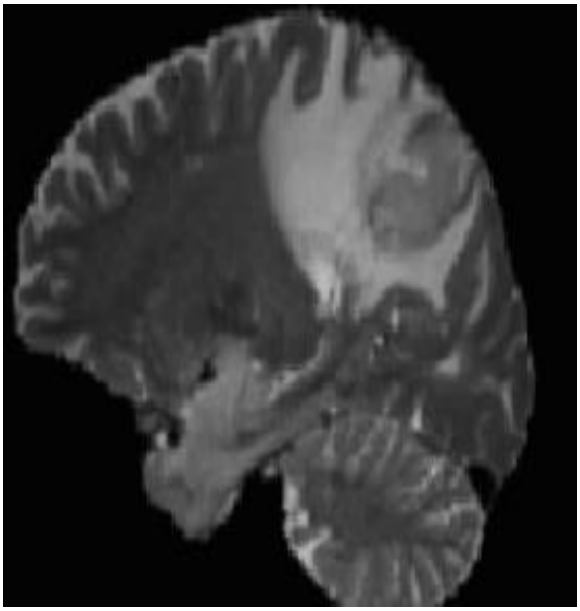

fig.70 shows the flair sagittal view.

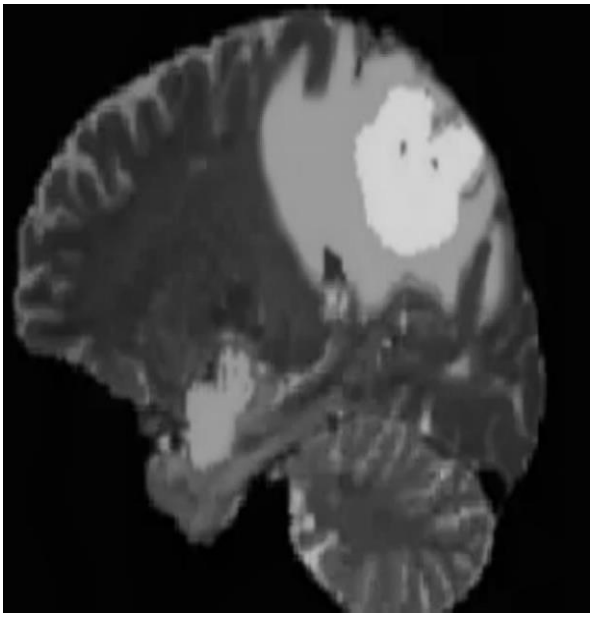

fig.71 shows the prediction sagittal view.

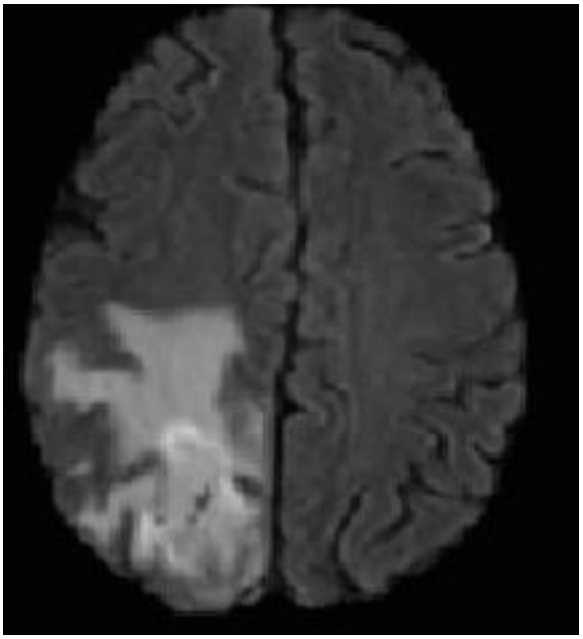

fig.72 shows the flair axial view.

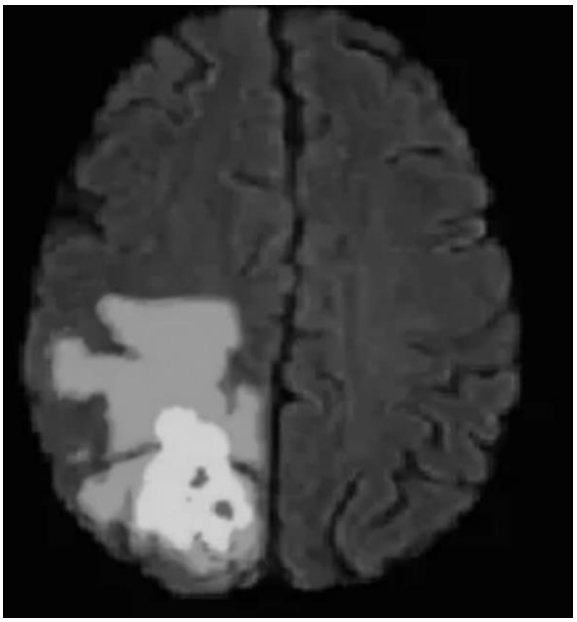

fig.73 shows the prediction axial view.

Convent brain segmentation based model graphs and results:

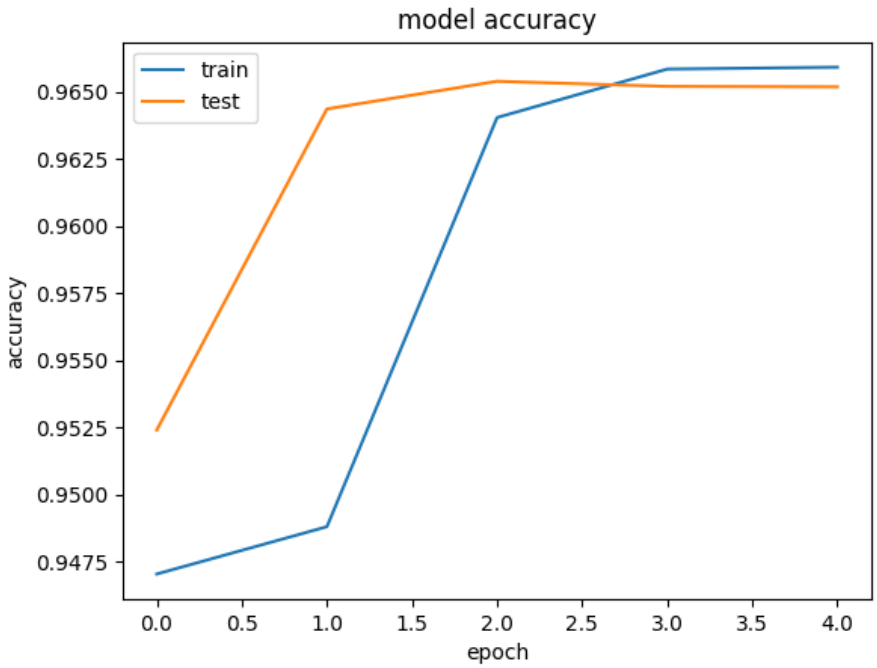

fig.74 shows the accuracy of the second model.

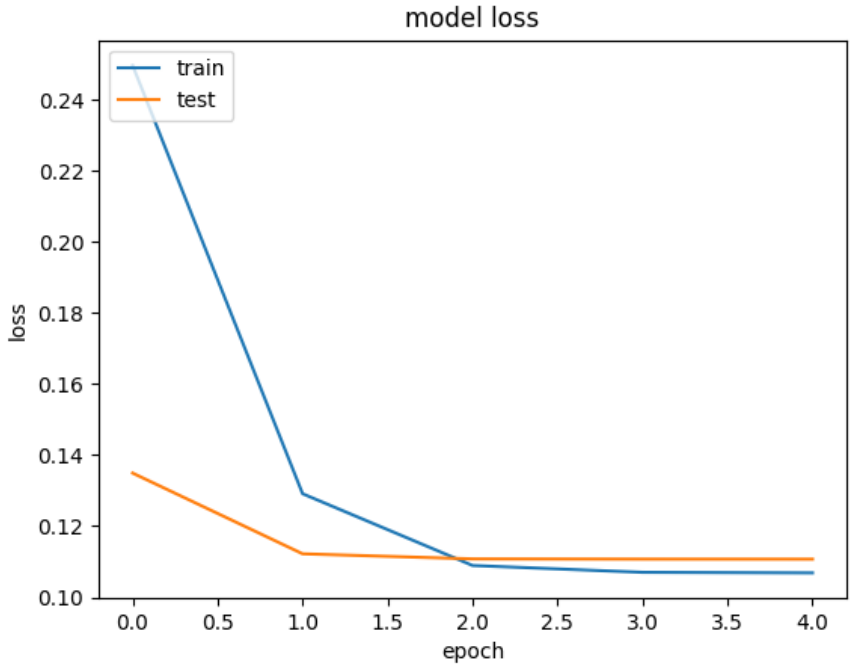

fig.75 shows the loss function of the second model.

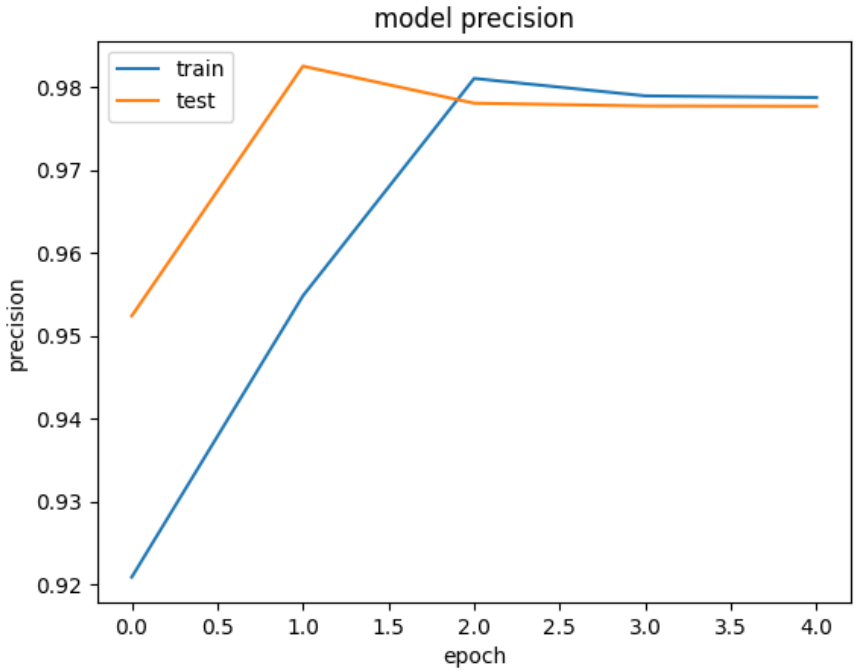

fig.76 shows the precision of the second model.

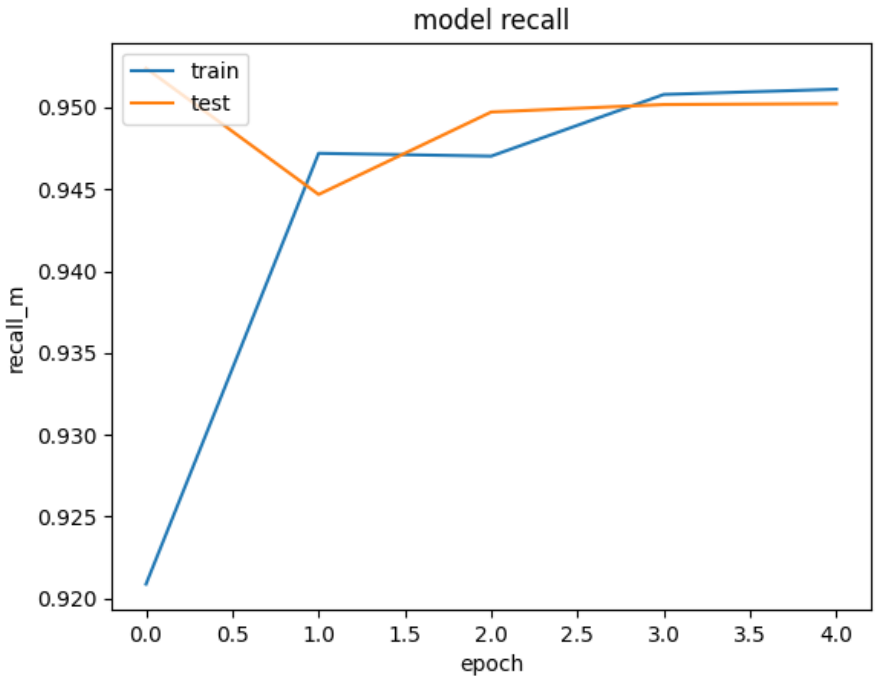

fig.77 shows the recall of the second model.

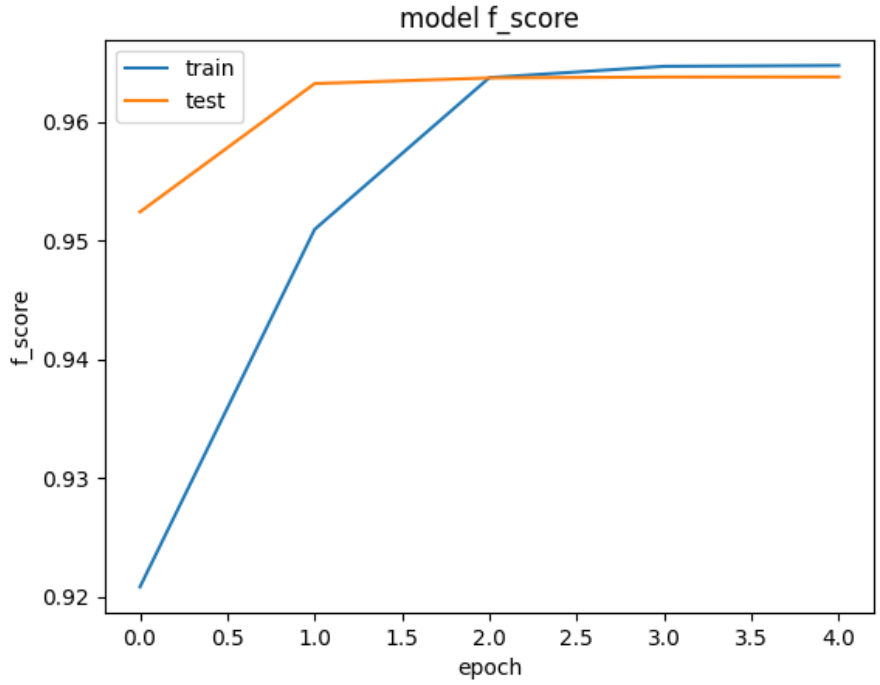

fig.78 shows the f_score of the second model.

5.2- classification analysis:

Due to the spreading of the tumors all over the world specially the dangers types of it like the brain tumor we try to help the specialists to solve this problem, but brain tumor problem is based on the segmentation of the tumor to help the specialists to detect the tumor place in the brain and give them the choose of how could they get this tumor out and give the perfect treatment to the condition so in this part we will show the results that we make for the classification of the tumor, we make a binary classifier for the problem that tell us If there is a tumor on this MRI image or not so the this is the simplest type of classifier that is not in the scope of the problem but we create it to make the problem so easy to solve and to tell the specialists if there is a tumor or not and if there is a tumor we represent the place and the tumor parts (core, enhanced tumor, edema) with a very low time and high performance that increase the quality of the medical care for all the patient and give all of them the opportunity to get a correct diagnoses for their problems and his will increase the chance to get better and recovery faster so this make the project more efficient faster more accurate and easy to use and we will show the results of this classification in the next figures:

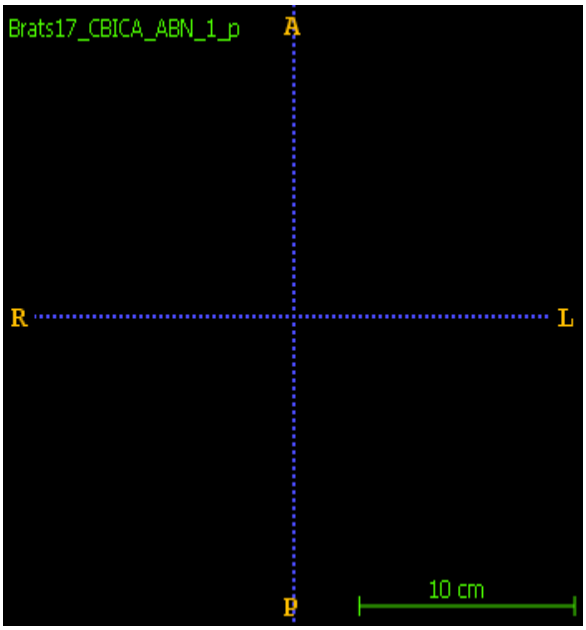

fig.79 shows this patent doesn't have tumor.

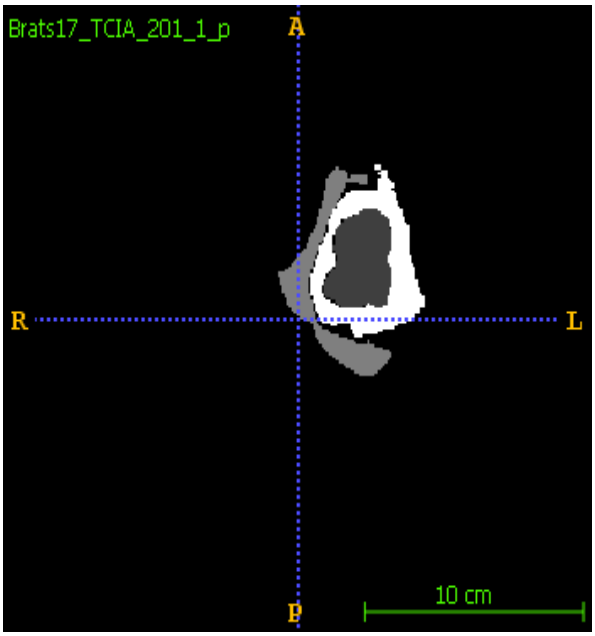

fig.80 shows patient has a tumor and this is its parts.

There are 4 levels of classification in the confusion matrix (no tumor, there is a tumor and this is its edema, enhanced tumor and tumor core) and the next figures shows them:

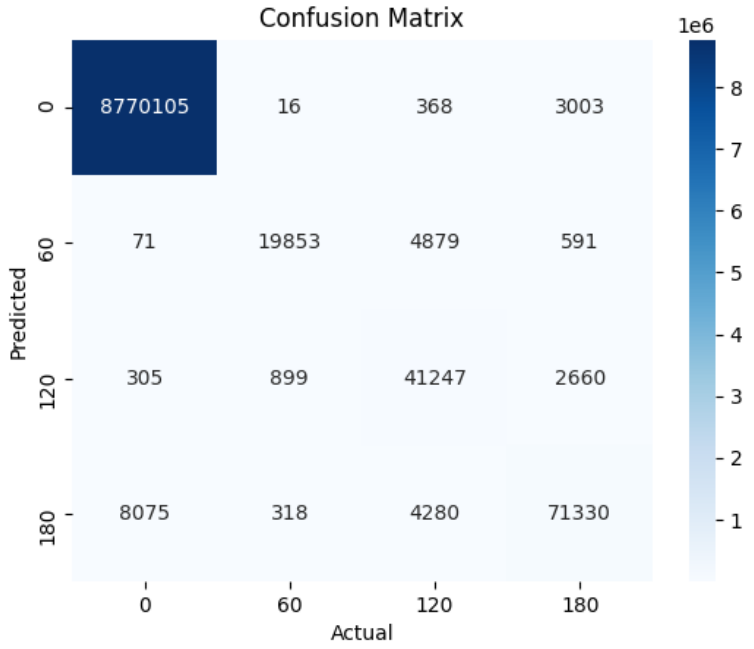

fig.81 shows the Confusion matrix of the first model

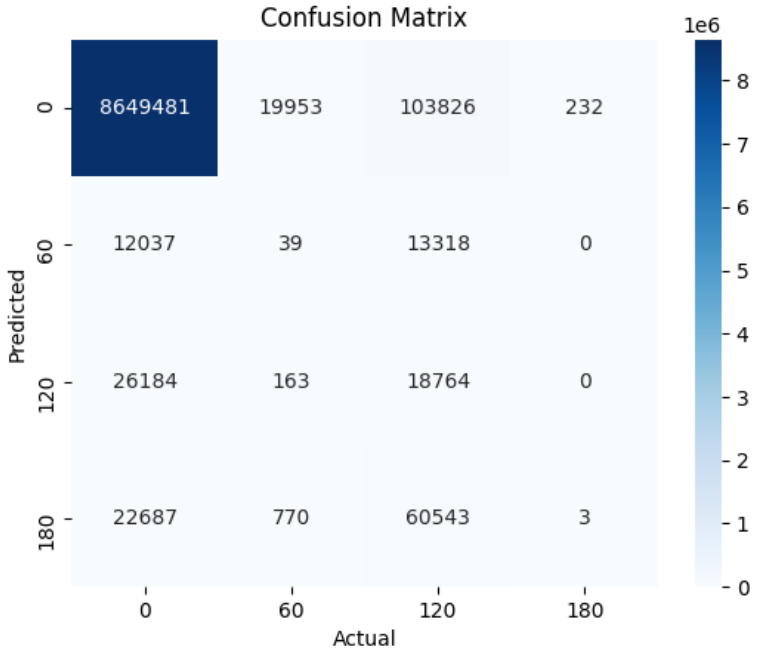

fig.82 shows the confusion matrix of the second model

5.3-implementation analysis:

This project is very complex and need a very good and power full hardware to get done so we use google Colab as an implementation tool for the two models and the specifications of the tool

1- 25 GB of Ram
2- 100 GB of storage
3- Nvidia K80 12 GB as a GPU for training the models

But google colab don’t fit all the dataset so its fit about 20% only so we are able to find another device more powerfull than google colab and use it to run the project.

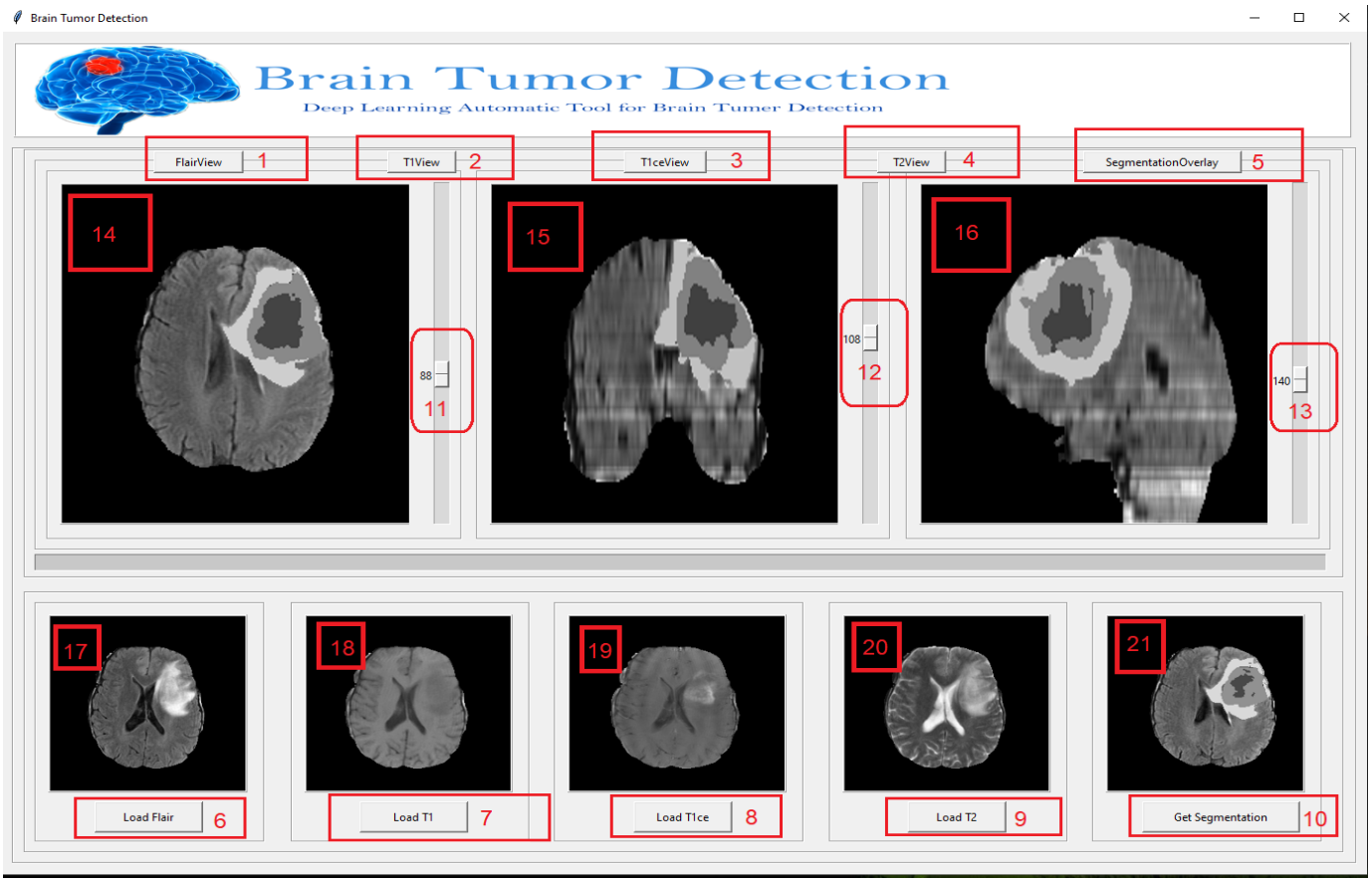

fig.83 shows the main screen from the project GUI.

The GUI parts:

Part (1, 2,3,4,5) for view the result of the different scans of the brain and the final prediction.

Part (6,7,8,9) for load the deferent scans of the brain

Part (10) for sun the application and get the prediction result.

Part (11,12,13) for scrolling the results to det deferent samples or slices

Part (14,15,16) for show 3 channels view for all the scans and final prediction

Part (17,18,19,20) for view the scans that we load

Part (21) for show the final result in one channel

5.4- comparative analysis:

In this chapter we will represent the final model accuracy and compare our two models with other models that solve the problem of brain tumor detection and the following table show this comparison:

Model Name	**Dataset**	**Accuracy**
Our first mode (U-net)	BraT's 2017, BraT's 2018	98.7 %
Our second model (convnet)	BraT's 2017, BraT's 2018	96.4 %
Survey on brain tumor detection	BraT's 2018	95.2 %
Automatic brain tumor segmentation	BraT's 2018	93.8 %
Multimodal Brain Tumor Segmentation Using Cascaded V-Nets	BraT's 2018	92.4 %
Tumor Segmentation and Survival Prediction in Glioma with Deep Learning	BraT's 2018	95.6 %
Segmentation of the Multimodal Brain Tumor Images Used Res-U-Net	BraT's 2020	96.1 %

Table. 1 shows the comparison between the different models

6. Conclusion

A fully automatic and accurate process is shown in this research, using a 2D deep convolution neural network with two different architectures based upon a well-known medical-image architecture for the segmentation of entire brain tumors and intra-tumor regions. The CNN model built has been trained in both the volumes HGG and LGG.

Both BraTS'2017 and BraTS'2018 training and challenge validation data sets have been tested and quantitatively analyzed.

The different tests have shown that the segmentation results have been quite successful with higher accuracy than other CNN models and evaluation actions have confirmed that our results are very comparable to those produced manually by the professionals, however the proposed approach can be further enhanced.

7. Future work

A more powerful GPU is proposed as future development to speed up CNN's learning phase further. A wider range of CNN topologies and other data increase approaches can therefore be tested. Other fascinating perspectives, for example stacking and blending in tumor core and active tumor areas, are also used to increase segmentation performance with ensemble learning approaches.

More accurate step that can be done in the future is classification which will help the medical staff to know not only the tumor location and region but also the grade of the tumor and the best treatment methods.

8.References

[1] Ronneberger, O., Fischer, P., Brox, T.: U-Net: convolutional networks for biomedical image segmentation. In: Navab, N., Hornegger, J., Wells, W.M., Frangi, A.F. (eds.) MICCAI 2015. LNCS, vol. 9351, pp. 234–241. Springer, Cham (2015). https://doi.org/10.1007/978-3-31924574-4_28

[2] He, K., Zhang, X., Ren, S., Sun, J.: Deep residual learning for image recognition. In: 2016 IEEE Conference on Computer Vision and Pattern Recognition (CVPR), pp. 770–778 (2016)

[3] He, K., Zhang, X., Ren, S., Sun, J.: Identity mappings in deep residual networks. In: Leibe, B., Matas, J., Sebe, N., Welling, Max (eds.) ECCV 2016. LNCS, vol. 9908, pp. 630–645. Springer, Cham (2016). https://doi.org/10.1007/978-3-319-46493-0_38

[4] He, K., Zhang, X., Ren, S., Sun, J.: Delving deep into rectifiers: surpassing human-level performance on ImageNet classification. In: Proceedings of the 2015 IEEE International Conference on Computer Vision (ICCV), pp. 1026–1034. IEEE Computer Society (2015)

[5] Milletari, F., Navab, N., Ahmadi, S.A.: V-Net: fully convolutional neural networks for volumetric medical image segmentation. In: 2016 Fourth International Conference on 3D Vision (3DV), pp. 565–571 (2016)

[6] Goodfellow, I., Bengio, Y., Courville, A.: Deep Learning. MIT Press, Cambridge (2016)

[7] Havaei, M., et al.: Brain tumor segmentation with Deep Neural Networks. Med. Image Anal. 35, 18 –31 (2017)

[8] ML \ CNN

https://www.ibm.com/cloud/learn/deep-learning

[9] Medical knowledge

https://www.mayoclinic.org/diseases-conditions/brain-tumor/symptoms-causes/syc-20350084#:~:text=A%20brain%20tumor%20can%20form,headaches%2C%20nausea%20and%20balance%20problems.

[10] Dataset description

https://www.med.upenn.edu/sbia/brats2018/data.html?fbclid=IwAR16uHBydL97in3Uld4hKbsIqiW_1B-IQKs4hJmgYrU63R2AaBIymI9ylYw

[11]https://www.academia.edu/9580212/A_PROJECT_REPORT_Submitted_by_Extracti_on_of_Tumor

[12]https://www.slideshare.net/Vivekreddy91/brain-tumor-detection-by-scanning-mri-images-using-filtering-techniques-79830026

[13]https://www.rcciit.org/students_projects/projects/ee/2020/GR15.pdf

[14]**https://github.com/naldeborgh7575/brain_segmentation**

[15]**https://github.com/sinAshish/Multi-Scale-Attention**

[16]**https://github.com/taigw/brats17**

[17]**https://github.com/charan223/Brain-Tumor-Segmentation-using-Topological-Loss**

[18]**https://github.com/deepmedic/deepmedic**

[19]**https://github.com/IAmSuyogJadhav/3d-mri-brain-tumor-segmentation-using-autoencoder-regularization**

[20]**https://github.com/jadevaibhav/Brain-Tumor-Segmentation-using-Deep-Neural-networks**

[21]**https://github.com/shalabh147/Brain-Tumor-Segmentation-and-Survival-Prediction-using-Deep-Neural-Networks**

[22]**https://paperswithcode.com/task/brain-tumor-segmentation**

[23]**http://www.ijstr.org/final-print/apr2020/A-Survey-On-Brain-Tumor-Detection-Based-On-Structural-Mri-Using-Machine-Learning-And-Deep-Learning-Techniques.pdf**

[24]**https://insightsimaging.springeropen.com/articles/10.1186/s13244-020-00869-4**

[25]**https://scholar.google.com.eg/scholar?q=Content-Based+Image+Retrieval+for+Detecting+Brain+Tumors+and+Amyl&hl=en&as_sdt=0&as_vis=1&oi=scholart**

[26] BRAIN_TUMOR_MRI_IMAGE_SEGMENTATION_AND_D.pdf

[27]**https://www.sciencedirect.com/science/article/abs/pii/S1361841516300330**

[28]**https://arxiv.org/abs/1705.03820**

[29]https://www.researchgate.net/publication/266411344_An_Efficient_Brain_Tumor_Detection_Algorithm_Using_Watershed_Thresholding_Based_Segmentation

[30]https://www.researchgate.net/publication/319623053_Identification_of_Brain_Tumor_using_Image_Processing_Techniques_-_Image_Pre-Processing_and_Segmentation

[31]https://www.med.upenn.edu/sbia/brats2017/data.html?fbclid=IwAR10_kAkmszZsFY7ceXOitlq_iUk8tqIlnju0u0ppFjkM76Q5X-5N7HutNU

[32]https://link.springer.com/chapter/10.1007/978-3-030-11726-9_4